

This document is downloaded from DR-NTU, Nanyang Technological University Library, Singapore.

Title	Neural-network-based smart sensor framework operating in a harsh environment
Author(s)	Patra, Jagdish Chandra; Ang, Ee Luang; Chaudhari, Narendra Shivaji; Das, Amitabha
Citation	Patra, J. C., Ang, E. L., Chaudhari, N. S., & Das, A. (2005). Neural-Network-Based Smart Sensor Framework Operating in a Harsh Environment. EURASIP Journal on Applied Signal Processing, 2005(4), 558-574.
Date	2005
URL	http://hdl.handle.net/10220/7115
Rights	© 2005 Jagdish C. Patra et al.

Neural-Network-Based Smart Sensor Framework Operating in a Harsh Environment

Jagdish C. Patra

*Division of Computer Communications, School of Computer Engineering, Nanyang Technological University, Singapore 639798
Email: aspatra@ntu.edu.sg*

Ee Luang Ang

*Division of Computer Communications, School of Computer Engineering, Nanyang Technological University, Singapore 639798
Email: aselang@ntu.edu.sg*

Narendra S. Chaudhari

*Division of Information Systems, School of Computer Engineering, Nanyang Technological University, Singapore 639798
Email: asnarendra@ntu.edu.sg*

Amitabha Das

*Division of Computer Communications, School of Computer Engineering, Nanyang Technological University, Singapore 639798
Email: asadas@ntu.edu.sg*

Received 11 February 2004; Revised 5 July 2004; Recommended for Publication by John Sorensen

We present an artificial neural-network- (NN-) based smart interface framework for sensors operating in harsh environments. The NN-based sensor can automatically compensate for the nonlinear response characteristics and its nonlinear dependency on the environmental parameters, with high accuracy. To show the potential of the proposed NN-based framework, we provide results of a smart capacitive pressure sensor (CPS) operating in a wide temperature range of 0 to 250°C. Through simulated experiments, we have shown that the NN-based CPS model is capable of providing pressure readout with a maximum full-scale (FS) error of only $\pm 1.0\%$ over this temperature range. A novel scheme for estimating the ambient temperature from the sensor characteristics itself is proposed. For this purpose, a second NN is utilized to estimate the ambient temperature accurately from the knowledge of the offset capacitance of the CPS. A microcontroller-unit- (MCU-) based implementation scheme is also provided.

Keywords and phrases: intelligent sensors, artificial neural networks, autocompensation.

1. INTRODUCTION

In many practical application areas of avionics, automobiles, robotics, missile guidance, oil drilling, and industrial measurements, sensors operate in harsh environments such as extreme ambient temperature, pressure, humidity, and so forth. In such situations, the response of the sensors depends not only on the measurand but also on the environmental parameters in a nonlinear manner. Usually, an exact mathematical model of a sensor showing the relationship between the measurand and its response, and its dependency on the environmental parameters, is not available. Further, since most of the sensors exhibit some amount of nonlinear response characteristics, and the environmental parameters influence the sensor behavior nonlinearly, the problem of obtaining an accurate readout and its calibration becomes more complex.

Some of the ideal properties of a sensor include linear response characteristics, autocorrection of the adverse effects of nonlinear environmental parameters, high sensitivity and accuracy, and low power consumption. However, in practical situations, it is not easy to achieve ideal sensor characteristics, especially when the sensor is operating in a harsh environment. In order to compensate for some of the nonidealities and to obtain accurate readout, several digital and analog interface circuits have been proposed in the past with some success [1, 2, 3, 4, 5, 6, 7]. These techniques include both iterative and noniterative algorithms, and involve complex analog and/or digital signal processing to model the sensor characteristics. They provide a limited solution to the complex problem under the assumptions that the range of variation of environmental parameters is small and that the influence of the environmental parameters on the sensor characteristics is linear.

Recently, artificial neural networks (NNs) have emerged as a powerful learning technique to perform complex tasks in dynamic environments. These networks are endowed with certain unique characteristics such as the capability of universal approximation, generalization, and fault tolerance. Because of these characteristics, there have been numerous successful applications of NNs in various fields of science, engineering, and industry [8, 9, 10]. It has been shown that the NN-based approximations to measurement data perform better than those of the classical methods of data interpolation and least mean square regression [11]. Application of NNs with superior performance for several instrumentation and measurement applications have been reported [12, 13, 14, 15, 16, 17, 18].

The main objective of this paper is to demonstrate the potential of NNs in the development of smart sensors capable of mitigating adverse effects of environmental parameters on the response characteristics of any type of sensor. For this purpose, we propose a multilayer perceptron (MLP)-based scheme to provide linear response characteristics with accurate pressure readout, and to compensate for the nonlinear temperature dependency of a capacitive pressure sensor (CPS) operating in a harsh environment with temperature variations from 0 to 250°C. We have assumed that the temperature influences the sensors's response characteristics nonlinearly and have performed simulation studies with three types of nonlinear dependencies.

An inverse model of the CPS is obtained by training a small-sized MLP using the popular backpropagation (BP) learning algorithm [8]. A small-sized MLP is preferable as the training time, computational complexity, and memory requirements decrease with the size of the MLP. To obtain ambient temperature information, a separate temperature sensor is usually embedded with the pressure sensor. An important contribution of this paper is that we have proposed a novel scheme to estimate the ambient temperature from the sensor characteristics itself, using a second MLP, thus eliminating the need of a separate temperature sensor. The performance of the NN-based scheme is compared with a polynomial-based interpolation scheme, and it is shown that the NN-based scheme outperforms the interpolation scheme.

The rest of the paper is arranged as follows. Section 2 presents a brief theoretical background of the CPS and the switched-capacitor interface (SCI). Section 3 provides details of the proposed MLP-based sensor modeling scheme. The simulated experiments are detailed in Section 4. Section 5 provides performance evaluation and discussions on results of these experiments. The performance comparison with a polynomial-based interpolation scheme is presented in Section 6. A microcontroller-unit-(MCU-) based implementation scheme is provided in Section 7, and finally, conclusions of the present study are drawn in Section 8.

2. CPS AND SCI

A CPS senses the applied pressure in the form of elastic deflection of its diaphragm. The capacitance of a CPS resulting

from the applied pressure P at the ambient temperature T is given by

$$C(P, T) = C_0(T) + \Delta C(P, T), \quad (1)$$

where $\Delta C(P, T)$ is the change in capacitance and $C_0(T)$ is the offset capacitance, that is, the zero-pressure capacitance, both at the ambient temperature T . The above capacitance may be expressed in terms of capacitances at the reference temperature T_0 as

$$C(P, T) = C_0 f_1(T) + \Delta C(P, T_0) f_2(T), \quad (2)$$

where C_0 is the offset capacitance and $\Delta C(P, T_0)$ is the change in capacitance, both at the reference temperature T_0 . The nonlinear functions $f_1(T)$ and $f_2(T)$ determine the effect of the ambient temperature on the sensor characteristics [3]. This model provides sufficient accuracy in determining the influence of temperature on the sensor's response characteristics.

When pressure is applied to the CPS, its change in capacitance at the reference temperature T_0 is given by

$$\Delta C(P, T_0) = C_0 P_N \frac{1 - \tau}{1 - P_N}, \quad (3)$$

where τ is the desensitivity parameter, P_N is the normalized applied pressure given by $P_N = P/P_{\max}$, and P_{\max} is the maximum permissible applied pressure. The parameters τ and P_{\max} depend on the geometrical structure and physical dimensions of the CPS.

In this study, in conformance with practical conditions, we have considered that the ambient temperature influences the CPS characteristics nonlinearly. The nonlinear functions involved are given by

$$f_i(T) = 1 + g_i(T), \quad (4)$$

$$g_i(T) = \kappa_{i1} T_n + \kappa_{i2} T_n^2 + \kappa_{i3} T_n^3, \quad (5)$$

where $T_n = (T - T_0)/T_{\max}$. The coefficients κ_{ij} , $i = 1, 2$, $j = 1, 2, 3$, determine the extent of nonlinear influence of the temperature on the sensor characteristics. Note that when $\kappa_{ij} = 0$ for $j = 2$ and 3, the influence of the temperature on the CPS response characteristics is linear. The maximum permissible temperature at which the sensor may be operated is denoted by T_{\max} . Let the normalized temperature T_N be given by $T_N = T/T_{\max}$. The normalized capacitance C_N may be expressed as

$$C_N = \frac{C(P, T)}{C_0}. \quad (6)$$

Using (2) and (3), this may be rewritten as

$$C_N = f_1(T) + \gamma f_2(T), \quad (7)$$

where $\gamma = P_N(1 - \tau)/(1 - P_N)$. Because of the requirement of the NN modeling, C_N in (7) is divided by a scale factor (SF) of 2, so as to keep its maximum value within 1. If the applied

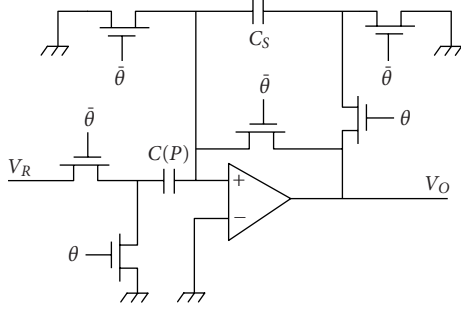


FIGURE 1: The switched-capacitor interface circuit.

pressure is zero, then γ becomes zero. Therefore, the normalized zero-pressure capacitance, that is, the normalized offset capacitance is given by

$$C_{N0} = f_1(T) = 1 + g_1(T). \quad (8)$$

SCI for the CPS is shown in Figure 1, where the CPS is represented by $C(P)$. The SCI output provides a voltage signal proportional to the capacitance change in the CPS due to the applied pressure. The SCI operation can be controlled by a reset signal θ . When $\hat{\theta} = 1$ (logic 1), $C(P)$ charges to the reference voltage V_R while the capacitor C_S is discharged to ground. On the other hand, when $\theta = 1$, the total charge $C(P)V_R$ stored in $C(P)$ is transferred to C_S producing an output voltage given by

$$V_O = K \cdot C(P), \quad (9)$$

where $K = V_R/C_S$. By choosing proper values of C_S and V_R , the normalized SCI output V_N may be obtained in such a way that

$$V_N = C_N. \quad (10)$$

The unnormalized and normalized SCI outputs at zero-applied pressure are denoted by V_{00} and V_{N0} , respectively. Therefore, if $P_N = 0$, then $V_{N0} = C_{N0}$.

3. THE MLP-BASED CPS MODEL

We propose an NN-based technique to obtain an inverse model of a CPS to provide accurate pressure readout under the nonlinear influence of the ambient temperature. The proposed scheme of the NN-based CPS model for the estimation of the applied pressure is shown in Figure 2. This scheme is analogous to the channel equalization scheme used in a digital communication receiver to cancel the adverse effects of the channel on the data being transmitted [8]. To obtain an accurate digital readout of the applied pressure, an MLP-based inverse model of the CPS is used to compensate for the adverse effects of the nonlinear characteristics and its variations due to the influence of the ambient temperature.

In this NN-based CPS model, all the signals used for training and testing are scaled by appropriate SFs to keep their range between 0 and 1. The model operates in two

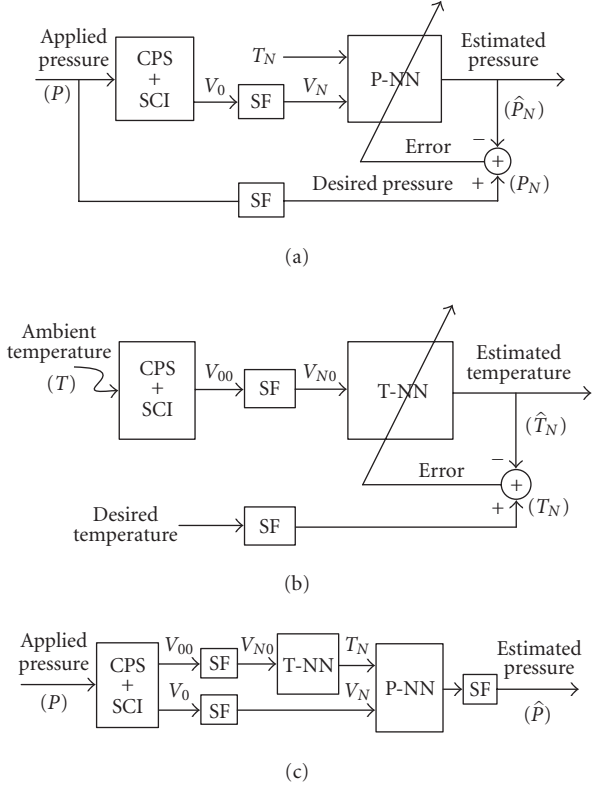


FIGURE 2: The scheme of NN-based modeling of a CPS. (a) Training phase: pressure. (b) Training phase: temperature. (c) Test phase: the complete model.

phases: the *training phase* and the *test phase*. In the *training phase*, the NNs used in the model are trained to learn the sensor characteristics and the environmental dependency. The pressure-NN (P-NN) is used to learn the sensor's response characteristics and its nonlinear dependency on the ambient temperature, whereas the temperature-NN (T-NN) is used to learn the nonlinear function representing variations in the ambient temperature.

We have used MLPs for both the P-NN and the T-NN. Several datasets are needed to train the NNs. An input pattern and its corresponding desired, or target pattern constitute one pair of data in the dataset. The available datasets are segregated into two parts. The first part, called *training set*, is used for training of the NNs, and the other part, called *test set*, is used to verify the effectiveness of the model.

3.1. Training phase: pressure

An MLP (P-NN) is used to learn the CPS response characteristics. The scheme for this is shown in Figure 2a. The inputs to the P-NN consist of the normalized temperature (T_N) and the normalized SCI output (V_N). The desired output is the normalized applied pressure (P_N). One dataset for a specific temperature is obtained by recording the SCI output (V_N) for different values of applied pressure, covering the operating range of the sensor. Next, at different temperature values, covering the full operating range, several datasets

are generated. The P-NN is trained by taking the patterns from the training set, and its weights are updated by using the popular BP algorithm [8]. After training, the weights of the NN are frozen and stored in an electrically erasable programmable read-only memory (EEPROM). In what follows, the final weights are denoted by W_P .

3.2. Training phase: temperature

A scheme to estimate the ambient temperature, by using another MLP (T-NN), only from the knowledge of the sensor characteristics is shown in Figure 2b. From (8), it may be seen that C_{N0} contains temperature information. However, since the influence of the temperature on the CPS characteristics is considered to be nonlinear, the temperature information cannot be obtained correctly from the knowledge of C_{N0} , using (8). The T-NN is trained by inputting the values of V_{N0} (the normalized SCI output corresponding to C_{N0} , that is, the SCI output at zero-applied pressure). The desired output is the normalized temperature T_N . Using the BP algorithm, the weights of the T-NN are updated. After the training is completed, the final weights are stored in an EEPROM. In what follows, the final weights are denoted by W_T .

3.3. Test phase: complete model

The complete scheme of the MLP-based model is shown in Figure 2c. In spite of the variation of the environmental temperature and its nonlinear influence on the CPS characteristics, this model can estimate the applied pressure accurately. During the *test phase* and actual use of the sensor, the weights W_P and W_T , stored in the EEPROM, are loaded into the P-NN and T-NN, respectively. The P-NN has learned the inverse characteristics of the CPS at different values of temperature, while the T-NN has learned the nonlinear function representing variations of the ambient temperature. The temperature information needed for the P-NN is obtained from the T-NN. The T-NN gets its input from the value of V_{N0} . Next, the input patterns from the test set are applied, and the model output (\hat{P}_N) is computed. If the model output matches closely with the actual applied pressure (P_N), then it may be said that the NN has learned the CPS characteristics correctly. Thereafter, the model can be used along with the CPS to estimate the pressure and to obtain its readout.

4. SIMULATION STUDIES

We carried out extensive simulation studies to evaluate performance of the proposed NN-based CPS model. In the following, we describe the details of the simulated experiments.

4.1. Preparation of datasets

All parameters of the CPS, such as, ambient temperature, applied pressure, and the SCI output voltage, used in the simulation study were suitably normalized to keep their values between 0 and 1. The datasets needed for training and testing of the NN were generated as follows. The SCI output voltage (V_N) was recorded at the reference temperature (25°C) at different known values of normalized pressure (P_N) chosen between 0.0 and 0.6 at an interval of 0.05.

TABLE 1: The values of κ_{ij} for linear and nonlinear forms of temperature dependencies.

NL form	κ_{11}	κ_{12}	κ_{13}	κ_{21}	κ_{22}	κ_{23}
NL0	-0.20	0.00	0.00	0.70	0.00	0.00
NL1	-0.20	0.20	-0.10	0.70	-0.30	0.40
NL2	-0.20	0.05	-0.20	0.70	-0.10	-0.50
NL3	-0.20	-0.10	-0.07	0.70	0.10	-0.30

Thus, these 13 pairs of data (P_N versus V_N) constitute one dataset at the reference temperature. To study the influence of temperature on the CPS characteristics, we have considered three forms of nonlinear functions denoted by NL1, NL2, and NL3, and a linear form denoted by NL0. These were simulated by choosing proper values of κ_{ij} in (5). The corresponding values of κ_{ij} are provided in Table 1.

Next, with the knowledge of the dataset at the reference temperature, and the chosen values of κ_{ij} , the response characteristics of the CPS for a specific ambient temperature were generated using (7). The response characteristics consist of 13 pairs of data (P_N versus V_N), and correspond to a dataset at that temperature. For a temperature range from 0°C to 250°C , at an increment of 10°C , twenty-six such datasets, each containing 13 data pairs, were generated. Next, these datasets were divided into two groups: the training set and the test set. The training set, used for training the NNs, consists of only five datasets corresponding to 0, 60, 120, 180, and 240°C , and the remaining twenty one datasets were used as the test set. Let the number of the datasets used for training and the number of data points in a dataset be denoted by N_{trgset} and N_{datpts} , respectively. In the following experiments, $N_{\text{trgset}} = 5$ and $N_{\text{datpts}} = 13$, and thus, the total number of training data points is 65 (13×5).

The response characteristics of the CPS for different values of temperature (0, 25, 80, 150, and 250°C) are shown in Figure 3. It may be observed that wide variation in the sensor characteristics occurs when the ambient temperature changes from 0°C to 250°C . Further, the sensor's response characteristics change differently for the linear form (NL0) and the three nonlinear forms (NL1–NL3) of temperature dependencies.

4.2. Training and testing of the P-NN

A 2-layer MLP with $\{2-4-1\}$ architecture was chosen in this modeling problem (see Figure 2a). Initially, all the weights of the P-NN were set to some random values within ± 1.0 . During training, a dataset was randomly selected from the five datasets, and a pattern from the selected dataset was also selected randomly. The initial values of the learning parameter α and the momentum factor β of the BP algorithm were chosen as 0.3 and 0.5, respectively. The MLP architecture and the values of α and β were selected after several experiments to provide optimum results.

Completion of weight adaptation of the 13 data pairs of all the five training sets constitute one iteration. For effective learning, 100 000 iterations were made to train the MLP model. To improve the learning, a variable learning

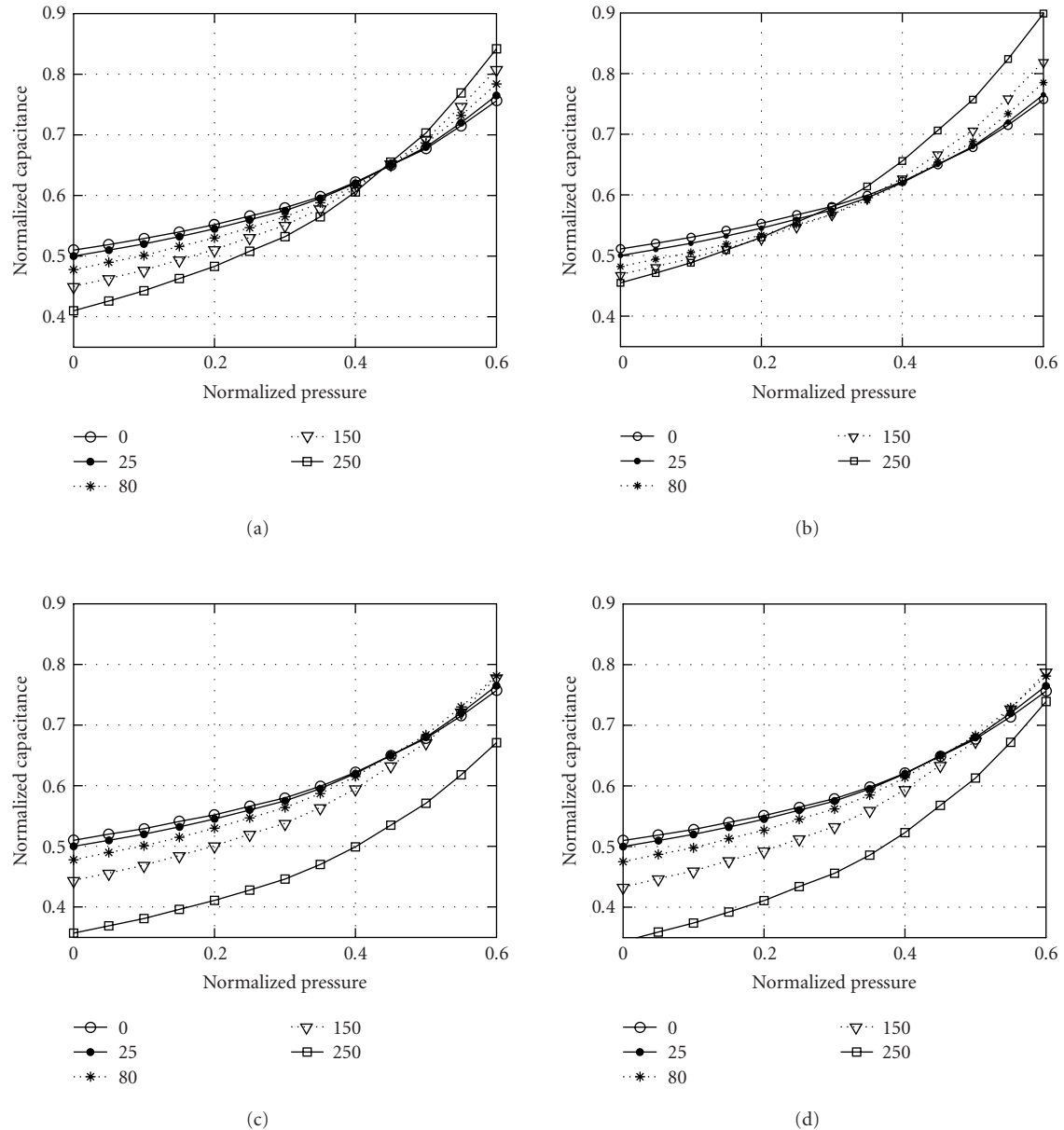


FIGURE 3: The response characteristics of the CPS operating at different temperatures (0, 25, 80, 150, and 250°C) with linear and three forms of nonlinear dependencies. (a) NL0. (b) NL1. (c) NL2. (d) NL3.

parameter was used in the BP algorithm. The learning parameter was varied as

$$\alpha_{ni} = \alpha_{ni-1} \left(1 - \frac{ni}{NITR} \right), \quad (11)$$

where ni is the current iteration number, and NITR is the total number of iterations used (in this case, NITR = 100 000). Using a Pentium 4, 2.8 GHz machine, it took only 13 seconds to train the MLP with 100 000 iterations. Finally, the weights of the P-NN (W_p) were stored for later use. This procedure was repeated for the linear (NL0) and the three nonlinear forms of temperature influences (NL1–NL3).

The four sets of the final weights (W_p) of the P-NN model are provided in Table 2.

Performance evaluation of the model was carried out by loading the final stored weights into the MLP. It is important to note that during the testing and actual use of the CPS model, updating of the weights does not take place. The NN estimates the applied pressure from the knowledge of the stored weights when the inputs are applied to the model. For the testing purpose, the SCI output voltage was varied from 0.35 to 0.90 with an increment of 0.001, and then applied to the model along with the temperature information. To evaluate the effectiveness of the model, the NN output (\hat{P}_N) was

TABLE 2: Final weights (W_P) of the P-NN ($\{2-4-1\}$ architecture). First layer: w_{ij} , $i = 1, 2, 3, 4$, and $j = 0, 1, 2$. Second layer: v_k , $k = 0, 1, \dots, 4$.

Weights	NL0	NL1	NL2	NL3
w_{10}	1.087	0.195	0.081	0.446
w_{11}	0.644	0.399	0.845	1.355
w_{12}	-0.938	-3.595	-0.697	-0.837
w_{20}	-1.912	-1.889	-1.965	-1.905
w_{21}	1.015	1.117	1.021	1.173
w_{22}	6.034	5.742	5.811	5.634
w_{30}	1.137	1.241	1.902	1.042
w_{31}	-0.548	-0.637	-1.511	-0.922
w_{32}	-1.497	-1.475	-0.262	-0.857
w_{40}	0.171	0.024	1.048	0.546
w_{41}	0.228	0.889	-0.486	0.659
w_{42}	-1.863	-0.567	-1.438	-2.110
v_0	-1.591	-2.184	-0.873	-1.026
v_1	-0.591	-0.945	-0.678	-0.483
v_2	2.094	1.813	1.776	1.723
v_3	-0.369	-0.543	-0.533	-0.667
v_4	-0.498	-0.550	-0.514	-0.227

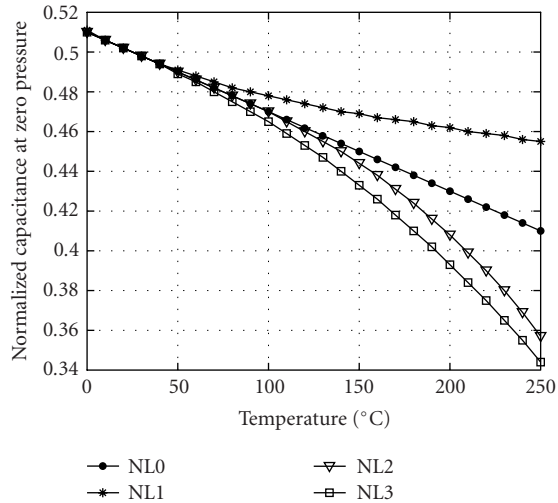


FIGURE 4: Variation of normalized offset capacitance (C_{N0}) of the pressure sensor with temperature for different forms of temperature dependencies.

computed and then compared with the true value of the applied pressure (P_N).

4.3. Training and testing of the T-NN

The T-NN was used to estimate the ambient temperature from the knowledge of C_{N0} at different temperatures. For the chosen values of κ_{ij} (see Table 1), the variation of C_{N0} with the change in temperature for the linear (NL0) and the three forms of nonlinear dependencies (NL1–NL3) are shown in Figure 4. The T-NN was employed to learn these nonlinear functions for estimating the ambient temperature.

TABLE 3: Final weights (W_T) of the T-NN ($\{1-4-1\}$ architecture). First layer: w_{ij} , $i = 1, 2, 3, 4$, and $j = 0$ and 1. Second layer: v_k , $k = 0, 1, \dots, 4$.

Weights	NL0	NL1	NL2	NL3
w_{10}	-2.277	0.347	-1.328	-0.439
w_{11}	4.070	-0.712	2.765	0.905
w_{20}	2.850	-12.661	0.048	-0.745
w_{21}	-4.611	30.122	-0.099	1.535
w_{30}	-3.558	-6.627	-1.594	-1.891
w_{31}	5.640	12.023	5.446	7.200
w_{40}	-4.577	-5.397	-4.005	-4.997
w_{41}	13.670	11.686	7.333	8.423
v_0	2.193	4.525	0.647	0.672
v_1	-0.137	0.004	-0.248	-0.021
v_2	0.490	-5.263	0.010	-0.027
v_3	-1.208	-0.952	-1.041	-1.607
v_4	-3.213	0.517	-0.911	-1.403

An MLP with $\{1-4-1\}$ architecture was chosen for this purpose. During training, the values of V_{N0} corresponding to 0, 60, 120, 180, and 250°C were chosen as the training set (the same temperature values were also used for training the P-NN). The input and desired output of the T-NN were the values of V_{N0} and T_N , respectively (see Figure 2b).

The initial values of both α and β were chosen as 0.7. The updating of the weights was carried out using the BP algorithm with a variable learning parameter over 200 000 iterations. Using a Pentium 4, 2.8 GHz machine, it took only 2 seconds to train the MLP with 200 000 iterations. The four sets of the final weights (W_T) corresponding to the linear and the three nonlinear forms of interaction are tabulated in Table 3.

Testing of the T-NN was carried out after loading the stored weights into the network. The V_{N0} was varied from 0.35 to 0.55 with an increment of 0.001 and then fed to the MLP. The output of the T-NN and the true value of the normalized temperature were compared to verify effectiveness of the model.

5. RESULTS AND DISCUSSIONS

Here, we provide the performance results of the simulation study for the estimation of the applied pressure and the ambient temperature.

5.1. Estimation of pressure

The true pressure and the pressure estimated by the MLP model at different values of temperature taken from the *test set* for the linear (NL0) and the three nonlinear forms (NL1–NL3) are plotted in Figure 5. Here, different symbols represent the true normalized pressure, while the dotted lines denote the estimated pressure. It may be noted that the P-NN has not seen the sensor characteristics for the temperature values of the test set. From this figure, it may be observed

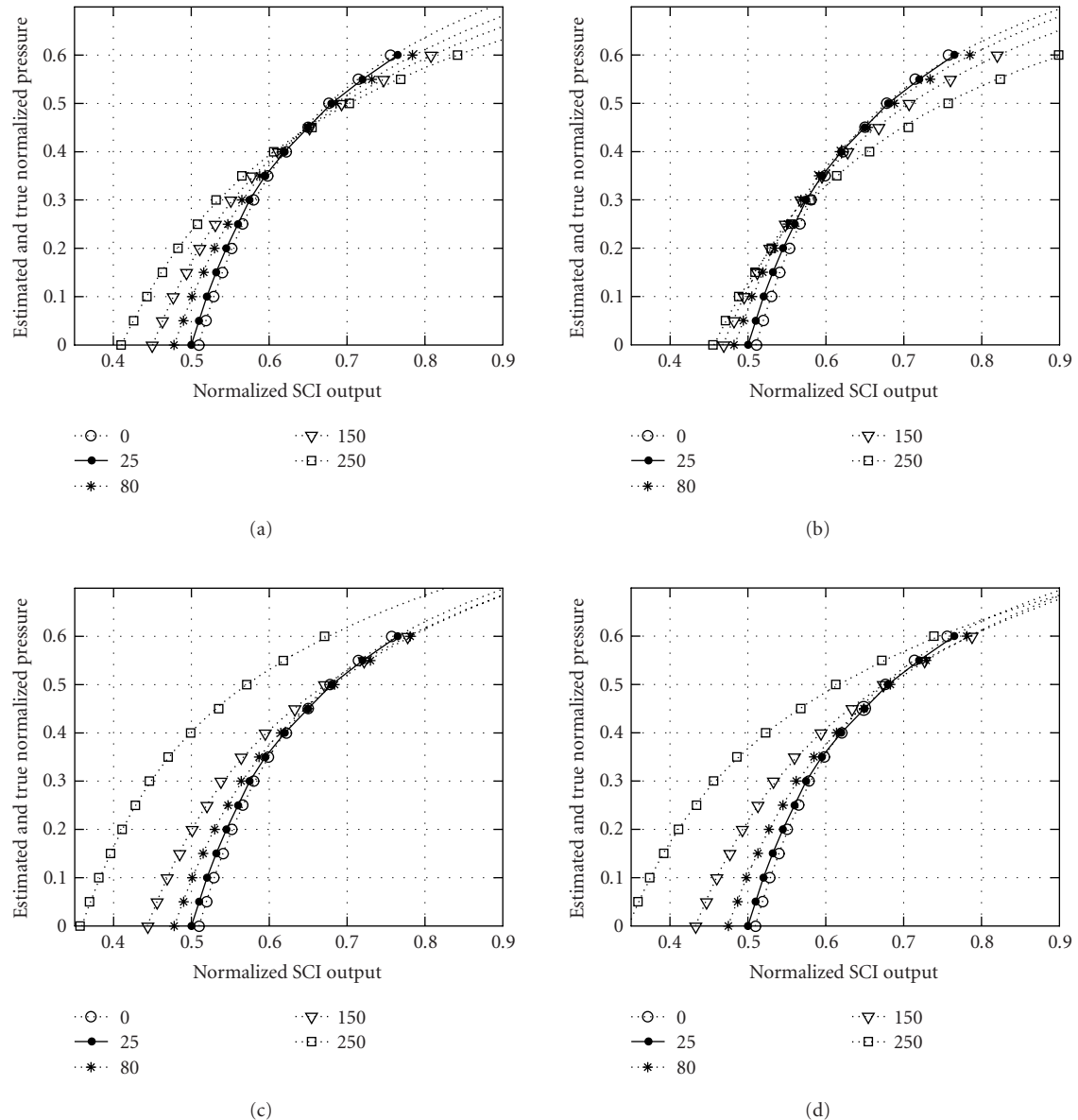


FIGURE 5: True response characteristics and the pressure estimated by the P-NN model of the CPS operating at different temperatures (0, 25, 80, 150, and 250°C) with linear and three forms of nonlinear dependencies. (a) NL0. (b) NL1. (c) NL2. (d) NL3.

that the MLP is capable of estimating the applied pressure accurately for the full range of applied pressure from 0.0 to 0.6. It is also capable of predicting the applied pressure for the range beyond 0.6, although the network was not trained for this range of P_N .

The full-scale (FS) percent error was computed as one hundred times the difference between the true pressure and the estimated pressure. The FS error at 0°C, 80°C, 150°C, and 250°C with the applied pressure varying from 0.0 to 0.6 for the four forms of temperature dependencies are plotted in Figure 6. Next, in Figure 7, we plotted the FS error for the whole temperature range from 0°C to 250°C, at specific values of applied pressure (i.e., $P_N = 0.1, 0.4, \text{ and } 0.6$),

for NL0 and NL1–NL3. The maximum FS error for the linear form NL0 remains within $\pm 0.75\%$, whereas, in the case of the three nonlinear forms, the maximum FS error remains within $\pm 1.0\%$.

5.2. Estimation of temperature

Plots of true temperature and the estimated temperature as a function of V_{N0} for the linear (NL0) and the three nonlinear forms (NL1–NL3) are shown in Figure 8. Here, the “dark dots” represent the true temperature and the dotted lines represent the temperature estimated by the T-NN model. Close agreement between the two values is evident from these plots.

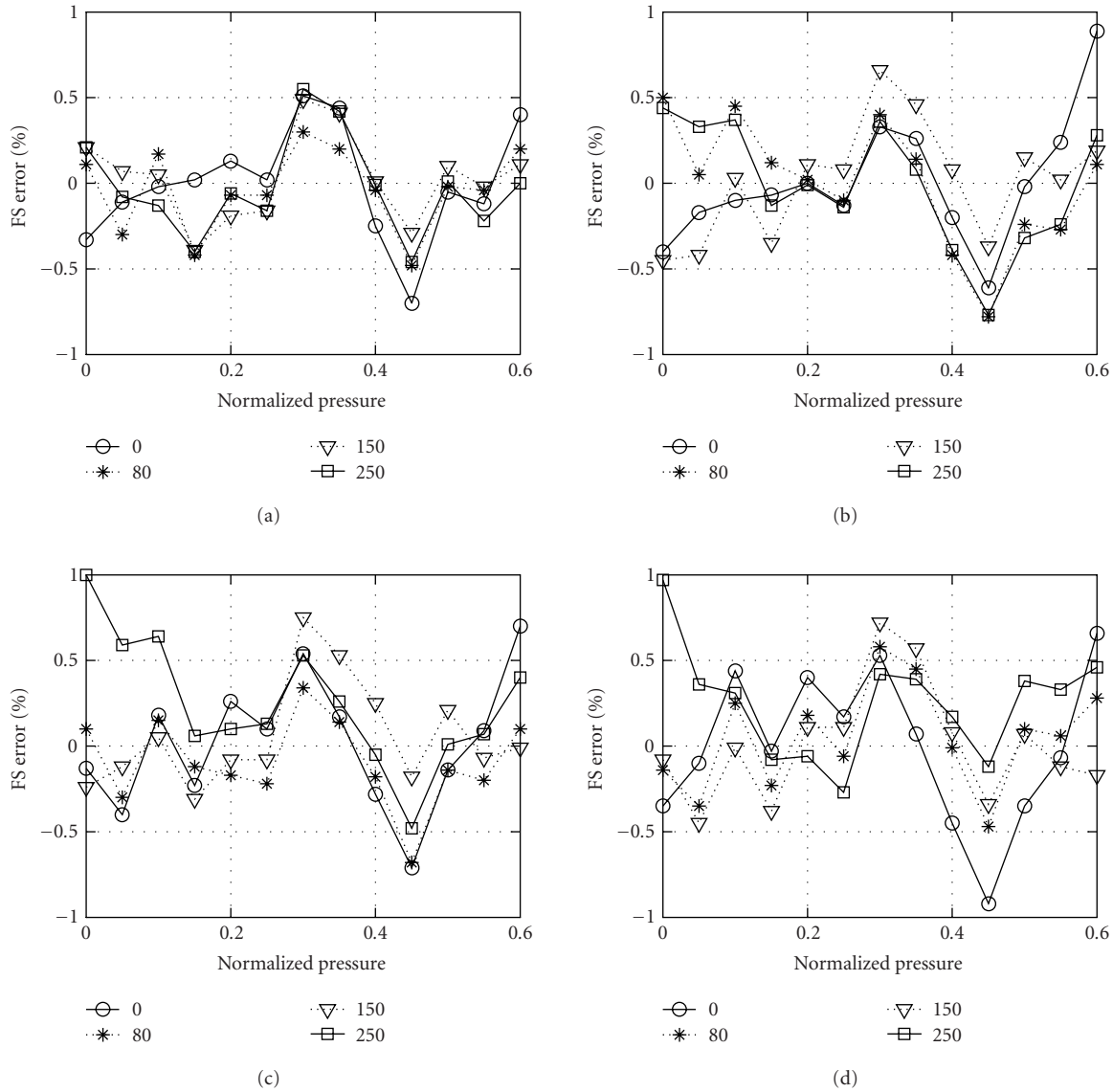


FIGURE 6: Full-scale percent error between the true and the estimated pressures at specific temperatures (0, 80, 150, and 250°C) with linear and three forms of nonlinear dependencies. (a) NL0. (b) NL1. (c) NL2. (d) NL3.

The FS percent error in estimation of the temperature for the four cases are plotted in Figure 9. For the whole range of temperature variation from 0°C to 250°C, the maximum FS error remains within $\pm 1\%$ for NL0, NL2, and NL3, and within $\pm 2\%$ for NL1. From these observations, effective performance of the T-NN is evident. Even though C_{N0} varies nonlinearly with temperature in different forms of nonlinear dependencies, the T-NN is able to estimate the ambient temperature accurately.

From the above findings, it may be concluded that the performance of the MLP model for the estimation of the applied pressure is excellent for the linear form of influence, and satisfactory for the three forms of nonlinear influences of temperature. In a similar application reported by Arpaia et al. [18], an MLP with 43 hidden layer nodes was used and a

maximum error of $\pm 2.4\%$ was obtained. In the present study, we have achieved a maximum error of only $\pm 1.0\%$ with a small-sized MLP of $\{2 - 4 - 1\}$ architecture (with only 17 weights). This is possible due to careful training of the MLP with the following strategies: (i) proper selection of initial learning rate and the momentum factor, (ii) use of a variable learning parameter (11), and (iii) application of randomly selected patterns from the training set.

The novelty of the proposed scheme is that even though the MLP was trained with patterns taken from only five temperature values (0, 60, 120, 180, and 240°C), it is capable of estimating the applied pressure accurately when the ambient temperature varies from 0°C to 250°C. Thus, the model is capable of effectively nullifying the nonlinear influence of the temperature on the CPS characteristics.

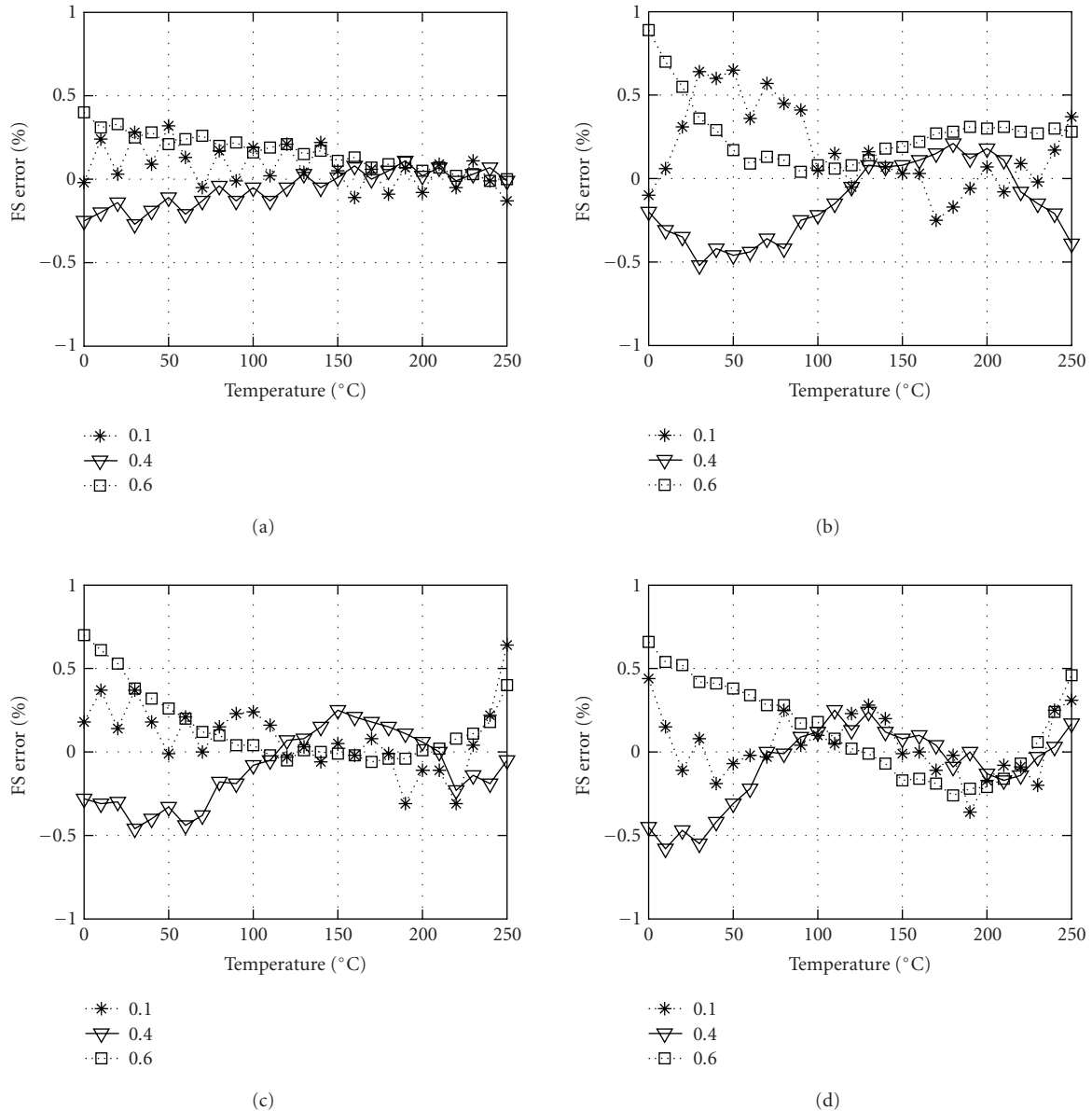


FIGURE 7: Full-scale percent error between the true and estimated pressures at specific normalized pressures ($P_N = 0.1, 0.4$, and 0.6) for the full range of variation of the ambient temperature. (a) NL0. (b) NL1. (c) NL2. (d) NL3.

6. AN INTERPOLATION SCHEME

Pereira et al. [11] have made extensive study on the relative performance of different methods in fitting a curve to sensor's dataset. Their dataset is one dimensional, that is, the sensor output (pressure readout) is a function of the SCI output. Using different interpolation methods, for example, Newton's, splines, polynomial, and NNs, they showed that the NN-based interpolation scheme outperforms other methods. When the data set is highly nonlinear, the NN-based scheme usually performs much better than the other methods. The main advantage of the NN-based curve fitting is its excellent extrapolation capa-

bility due to nonlinear processing of multivariate data. After successful training of the NN, it provides lower errors outside the calibration range of the sensor than the polynomial extrapolation. Relative performance of different methods of curve-fitting techniques are provided in Table 4 (taken from [11]). Here, the "Poly. Degree" values for the NN row correspond to the number of hidden layer nodes.

We present a polynomial-based interpolation scheme of data fitting of 2D sensor data, and compare its performance with the NN-based model. Here, the sensor data has two independent variables: ambient temperature (x_1) and normalized SCI output (x_2), and the output variable is the estimated

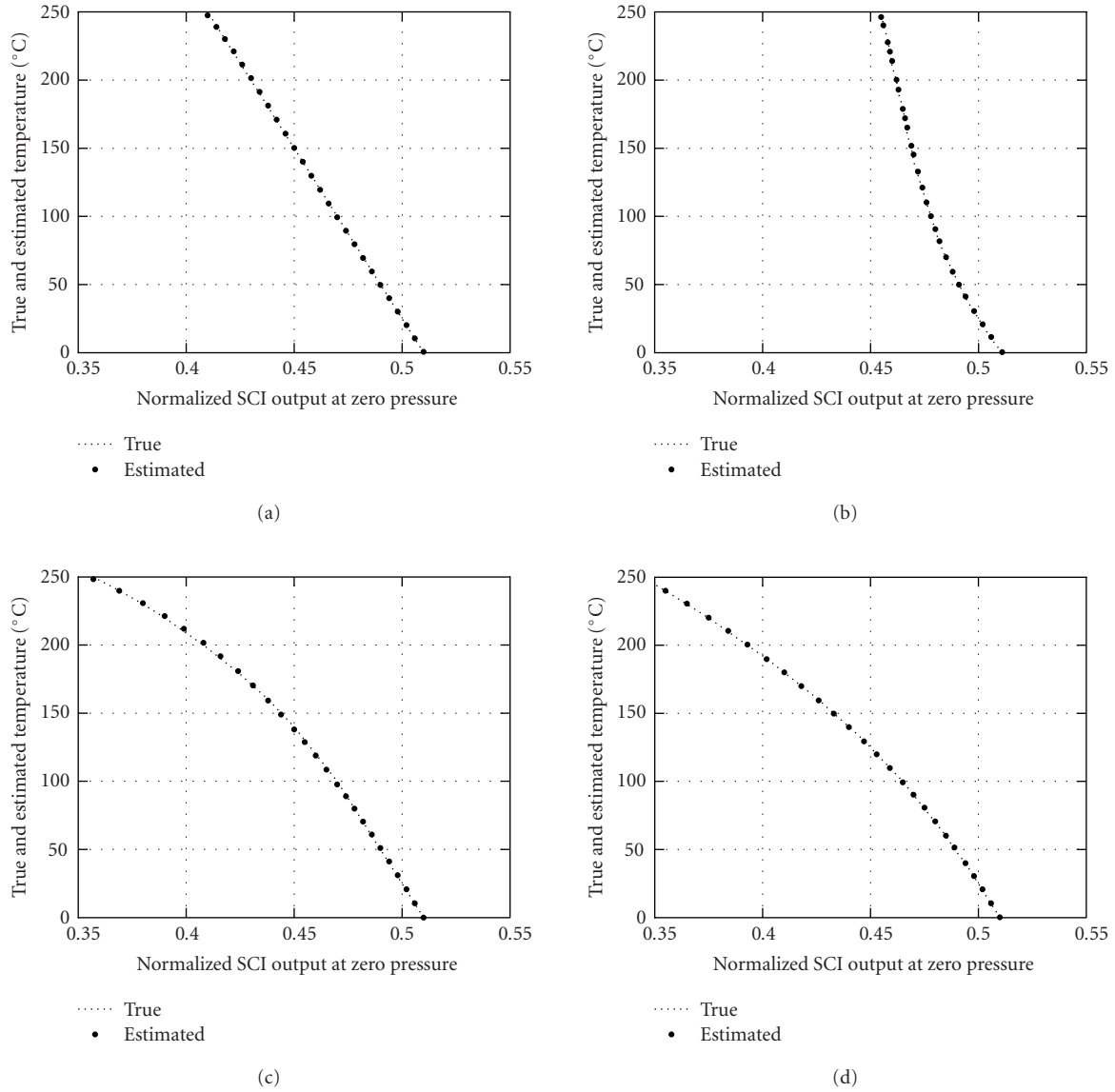


FIGURE 8: The true temperature and the estimated temperature by the T-NN model with linear and three forms of nonlinear dependencies. (a) NL0. (b) NL1. (c) NL2. (d) NL3.

pressure (y). Let the polynomial model of the sensor be given by

$$y = a_0 + \sum_{j=1}^J a_j x_1^j + \sum_{j=1}^J b_j x_2^j + \sum_{j=1, k=1, j+k \leq J}^{J-1} c_{jk} x_1^j x_2^k, \quad (12)$$

where J is the polynomial degree, and a_j , b_j , and c_{jk} are the coefficients of the model to be determined. The dataset consists of 13×5 measurement points corresponding to 13 measurements for each of the five temperature values of 0, 60, 120, 180, and 240°C. Using Gauss-Newton method, the training data was fitted with the polynomial model. The coefficients of the model are estimated by least squares method.

The average mean square error (MES) between the true and estimated pressures is defined as

$$\text{MSE}_{\text{avg}} = \frac{1}{N_{\text{td}}} \sum_{j=1}^{N_{\text{trgset}}} \sum_{k=1}^{N_{\text{datpts}}} (P_{\text{tru}}(j, k) - P_{\text{est}}(j, k))^2, \quad (13)$$

where $N_{\text{td}} = N_{\text{trgset}} \times N_{\text{datpts}}$, $N_{\text{trgset}} = 5$ for the five temperature values, $N_{\text{datpts}} = 13$ for the thirteen measurements, P_{tru} is the true pressure, and P_{est} is the estimated pressure by the model. The MSE_{avg} in dB for different degrees of polynomial model and the P-NN model (using Table 2) were computed and are tabulated in Table 5. The values in the last row of this table indicate the number of coefficients/weights in the model. It can be seen that the MSE_{avg} improves as the

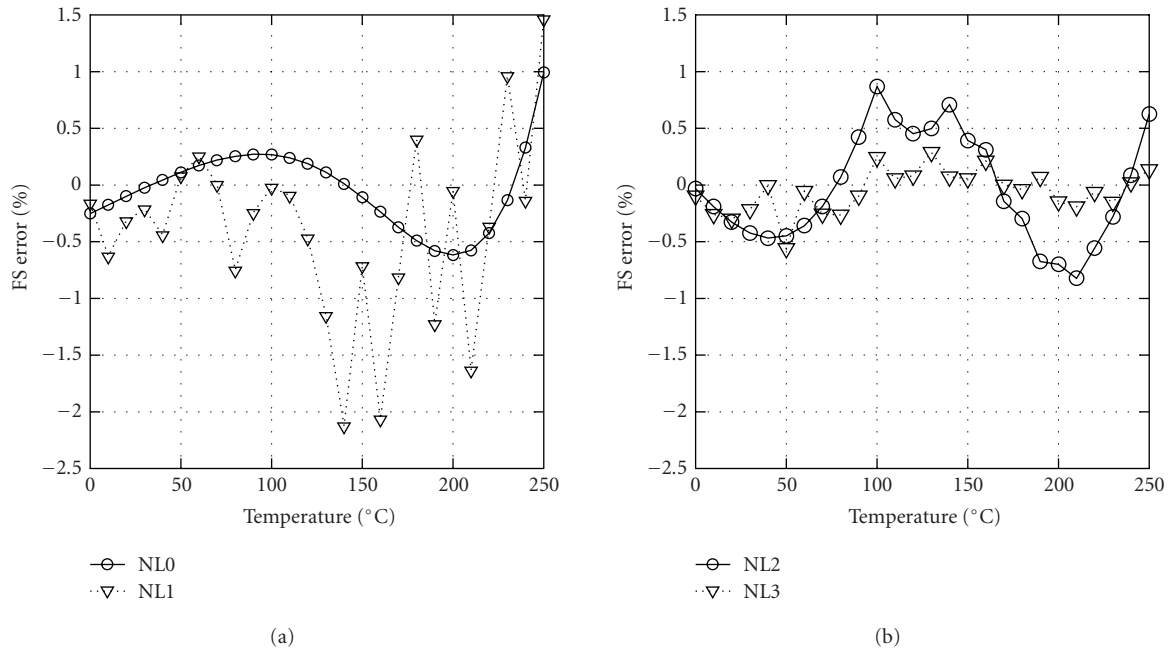


FIGURE 9: Full-scale percent error in estimation of temperature by the T-NN model with linear and three forms of nonlinear dependencies. (a) NL0 and NL1. (b) NL2 and NL3.

TABLE 4: Relative performances of different methods in fitting a curve to a dataset. The “Poly. deg.” values for the NN row correspond to the number of hidden layer nodes (taken from [11]).

Methods	No. of points	Max. rel. error(%)	Poly. deg.	$\sigma \times 10^{-2}$
Newton's	10	11.5	9	1.7
	15	31.2	14	5.6
Splines	10	14.2	3	2.3
	15	11.6	3	1.7
Polynomial	10	11.5	9	1.8
	15	9.6	9	1.3
NN	10	4.8	6	0.96
	15	4.5	5	1.0

TABLE 5: The MSE_{avg} for different degrees of the polynomial model and the NN model with $N_{trgset} = 5$. The last-row values indicate the number of coefficients/weights in the model.

NL form	$J = 3$	$J = 4$	$J = 5$	NN model
NL0	-43.40	-45.35	-46.99	-51.83
NL1	-41.92	-44.75	-46.77	-49.67
NL2	-46.87	-46.72	-46.51	-50.42
NL3	-45.17	-46.07	-46.55	-49.73
	10	15	21	17

degree of the polynomial model is increased. However, for $J > 5$, there is no substantial improvement in the MSE_{avg} of the polynomial model. The MSE_{avg} for the P-NN model is found to be less than that of the polynomial model for the linear (NL0) and the three nonlinear temperature dependencies (NL1–NL3).

The estimated coefficients for the linear (NL0) and the three nonlinear temperature dependencies (NL1–NL3) for the polynomial model of degree of five ($J = 5$ with 21 coefficients) are provided in Table 6. All subsequent comparisons are made based on this polynomial model.

The FS percent error for the polynomial model ($J = 5$) at specific normalized pressure values covering the entire temperature range are plotted in Figure 10. Similar plots for the P-NN model are shown in Figure 7. Comparing these two figures, one can see that the FS percent error for the P-NN model is less than that of the polynomial model for the linear (NL0) and the three nonlinear dependencies (NL1–NL3).

As stated earlier, the prime advantage of the NN model is its superior extrapolation capability compared to other models. To study the extrapolation capability, we carried out several experiments with the NN model and the polynomial interpolation model using the linear (NL0) and nonlinear

TABLE 6: The estimated coefficients of the polynomial model ($N_{\text{trgset}} = 5$ and $J = 5$) for linear (NL0) and three nonlinear temperature dependencies (NL1–NL3).

Coefficients	NL0	NL1	NL2	NL3
a_0	-6.769	-7.169	-6.115	-6.264
a_1	6.131	6.128	3.762	5.280
a_2	-1.048	-2.124	-0.905	-0.271
a_3	-0.065	0.750	0.458	-0.238
a_4	0.371	1.197	0.619	0.006
a_5	-0.158	-0.547	-0.322	-0.085
b_1	21.018	22.918	18.131	18.659
b_2	-11.521	-14.165	-8.085	-8.437
b_3	-10.327	-10.570	-9.516	-9.837
b_4	3.417	6.349	0.109	0.225
b_5	5.699	4.168	6.886	7.092
c_{11}	-16.218	-16.023	-7.766	-13.322
c_{21}	-0.480	1.124	1.411	-0.658
c_{12}	5.169	4.642	-0.509	3.443
c_{31}	-0.471	-4.175	-2.052	0.637
c_{22}	7.691	9.150	0.494	3.641
c_{13}	13.921	14.949	6.551	10.717
c_{41}	0.036	0.122	0.111	0.338
c_{32}	0.152	2.385	1.475	-0.747
c_{23}	-6.580	-8.381	-0.843	-2.712
c_{14}	-9.029	-9.982	-1.621	-5.865

(NL1–NL3) temperature dependencies. From the original training dataset, the 13 data points corresponding to 240°C were removed. Thus, the training data consists of 13×4 data points corresponding to 13 data points from each of 0, 60, 120, and 180°C ($N_{\text{trgset}} = 4$).

The NN model, P-NN, was trained with these datasets and a set of weights were obtained for each of the linear (NL0) and nonlinear dependencies (NL1–NL3). Similarly, with a polynomial degree of 5 ($J = 5$), a set of coefficients of the polynomial model were estimated by using Gauss-Newton method with least squares (for NL0–NL3). The applied pressure was estimated by the P-NN model and the polynomial model using P-NN weights and polynomial coefficients, respectively. The FS error between the true and the estimated pressures at specific temperature values of 210, 220, 230, and 240°C for the linear (NL0) and nonlinear temperature dependencies (NL1–NL3) are plotted in Figure 11. In this figure, the top row corresponds to the NN model and the bottom row corresponds to the polynomial model.

It may be noted that both the P-NN model and the polynomial model have seen data covering only temperatures from 0°C to 180°C. From Figure 11, superior performance of the P-NN model over the polynomial model for temperature range of 210°C–240°C is evident. In particular, for the linear dependency (NL0), the FS error of the P-NN model remains within $\pm 1\%$ (similar to that of the previous case). However, for nonlinear dependencies (NL1–NL3), the maximum FS error remains between +5% and -2%. On the other hand, in the case of the polynomial model, as the tempera-

ture increases from 210°C to 240°C, the FS error increases from -3% to -10% for the linear dependency (NL0). The performance for NL1 is the worst for the polynomial model. As the temperature increases from 210°C to 230°C, the FS error increases from -5% to -12%, and it becomes more than -15% at 240°C. For NL2 and NL3, the maximum FS error remains within -13% and -8%, respectively.

Performance comparison between the P-NN model and the polynomial model for the entire range of temperature at specific values of normalized pressure are plotted in Figure 12. In this figure, the top row corresponds to the P-NN model while the bottom row corresponds to the polynomial model. Superior extrapolation capability of the P-NN model is evident in this figure. For the entire range of temperature (0°C – 250°C), the FS error for linear dependency (NL0) remains within $\pm 1\%$ for the P-NN model. For the temperature range from 0°C to 200°C, the FS error is larger in the polynomial model compared to that in the P-NN model. Beyond 200°C, the performance of the polynomial model is much worse than the P-NN model for the linear and nonlinear dependencies (NL0–NL3).

The average MSE, MSE_{avg} , in dB was computed for the P-NN model and the polynomial interpolation model ($N_{\text{trgset}} = 4$ and $J = 5$) and are provided in Table 7. For the temperature range from 0°C–250°C, in comparison to Table 5 ($N_{\text{trgset}} = 5$ and $J = 5$), a substantial degradation of MSE_{avg} can be seen for the polynomial model. On the other hand, although there is a degradation for the NN model, it is not severe. In particular, in the case of the P-NN model there is not much change in the MSE_{avg} for the linear dependency (NL0) compared with the previous case (Table 5).

For the temperature range from 0°C – 200°C, the MSE_{avg} is comparable to that of Table 5 for both the P-NN and polynomial models. This fact indicates that the performance of the polynomial model is satisfactory for interpolation, but its performance severely deteriorates in the case of extrapolation, whereas the performance of the NN model is found to be superior than the polynomial model for both interpolation and extrapolation of the sensor data.

7. AN IMPLEMENTATION SCHEME

Due to the rapid decrease in unit cost and fast increase in on-chip capabilities, MCUs have been used in various intelligent embedded systems. An implementation scheme of the MLP-based CPS model using an MCU is depicted in Figure 13. The SCI converts the change in capacitance of the CPS due to the applied pressure into an equivalent voltage level. This analog SCI output voltage is passed through an analog-to-digital converter (ADC). The digital temperature information is similarly obtained from the knowledge of V_{N0} (i.e., the SCI output when the applied pressure is zero). During the training phase, the CPS is operated at a controlled temperature and the data pairs are collected for the training set data. These training data are fed to a personal computer (PC) connected to the MCU for the training of the MLP-based model. After completion of the training, the weights of the

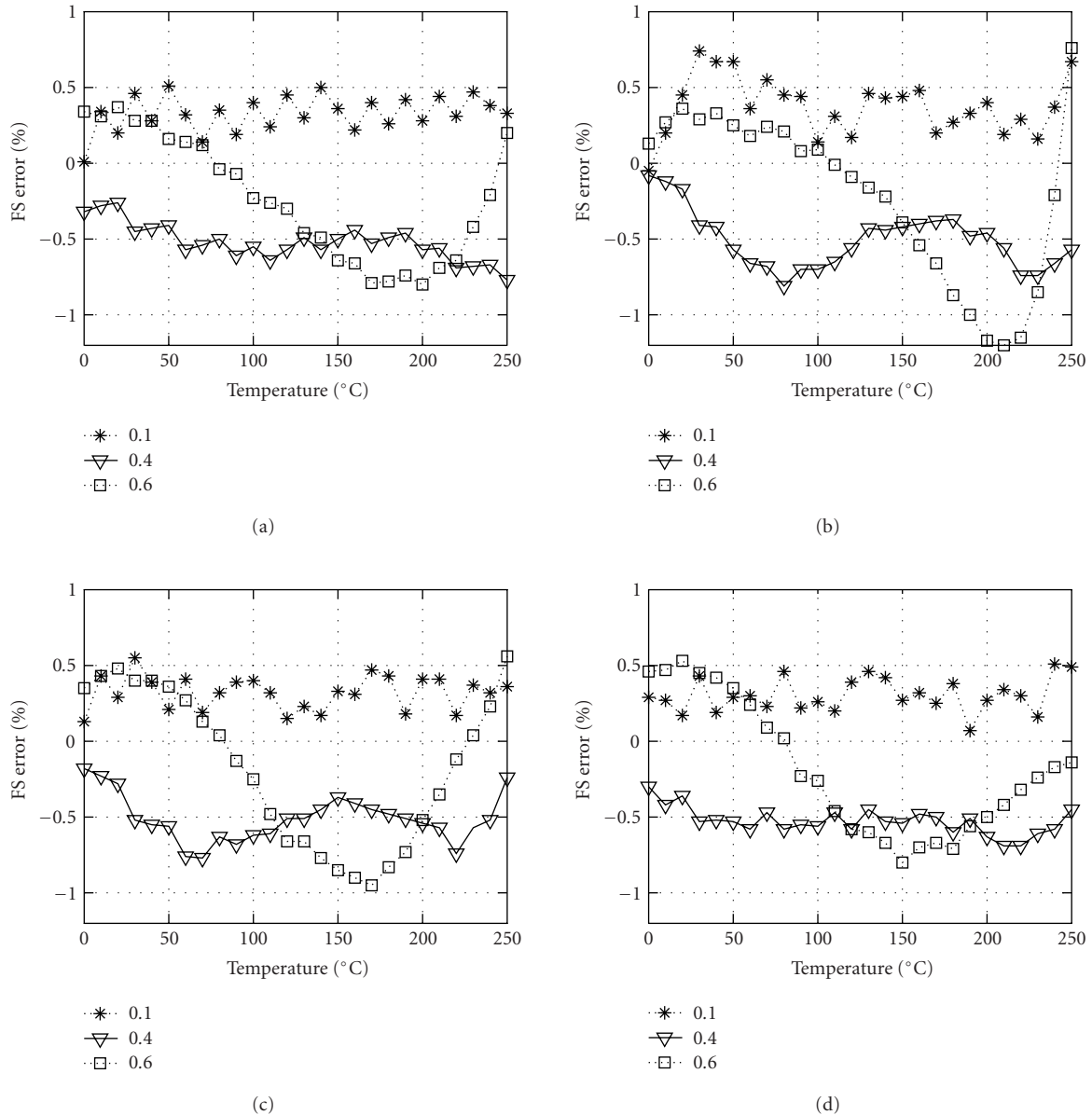


FIGURE 10: Full-scale percent error between the true and estimated pressures for the polynomial model ($J = 5$) at specific normalized pressures ($P_N = 0.1, 0.4$, and 0.6) with full range of variation of the ambient temperature. (a) NL0. (b) NL1. (c) NL2. (d) NL3.

MLP are stored in the EEPROM of the MCU. With the available hardware, such as adders and multipliers of the MCU, the MLP-based model can be implemented and the digital readout of the applied pressure can be displayed through the bus interface circuit.

To estimate the ambient temperature from the sensor characteristics itself, we propose the following scheme. In practical use of a CPS, there is only one output signal (the SCI output V_N) corresponding to the measurand (applied pressure). Therefore, appropriate provisions are to be made to obtain the signals separately for estimation of the temperature and the pressure. The online estimation of pressure using the NN-based scheme can be carried out in a measure-

ment phase which consists of one t_{est} and one p_{est} cycle. In the t_{est} cycle, the ambient temperature is estimated, whereas in the p_{est} cycle the applied pressure is estimated.

During t_{est} cycle, provision is made to separate the CPS from the applied pressure, and the SCI output V_{N0} corresponding to the zero pressure is then recorded. From the knowledge of V_{N0} , the ambient temperature can be estimated using the T-NN. Next, during the p_{est} cycle, the pressure is applied to the CPS, and the SCI output V_N is recorded. Now, using the recorded values of V_{N0} and V_N , the applied pressure can be estimated using the NN models as shown in Figure 2c. Appropriate control and logic circuits are to be incorporated with the MCU for this measurement scheme.

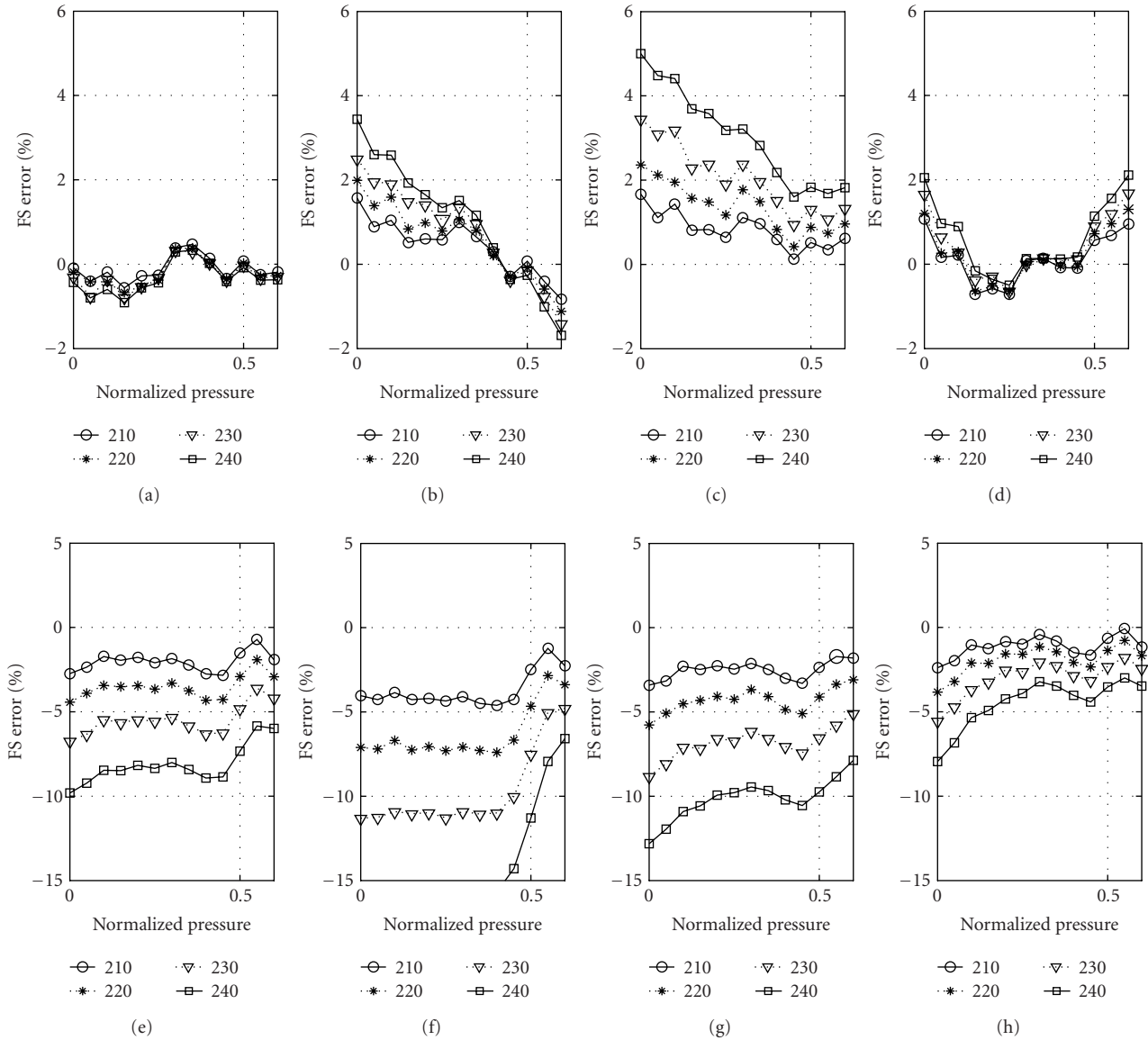


FIGURE 11: Full-scale percent error between the true and estimated pressures at specific temperatures (210, 220, 230, and 240°C) with different forms of nonlinear dependencies. (a) and (e) NL0; (b) and (f) NL1; (c) and (g) NL2; and (d) and (h) NL3. The top row corresponds to the NN model and the bottom row corresponds to the polynomial model ($J = 5$). Both models were trained with $N_{\text{trgset}} = 4$.

However, if the environmental temperature variation is not frequent, then the t_{est} cycle need not be carried out in each measurement phase, but only at regular intervals. The estimated temperature of the preceding t_{est} cycle (saved in the RAM of the MCU) can be used to estimate the applied pressure in the current measurement phase.

8. CONCLUSIONS

Smart sensors operating in harsh environments should be capable of providing accurate readout and autocompensation of the nonlinear influence of the environmental parameters on its response characteristics. For this purpose, we have proposed a novel NN-based technique for mod-

eling a CPS operating in a harsh environment in which the temperature can vary from 0 to 250°C. Using a variable learning rate BP algorithm and taking random samples during training, a highly effective NN-based CPS model was obtained. A compact MLP of $\{2 - 4 - 1\}$ architecture (with only 17 weights) is capable of providing accurate pressure readout. Using a second MLP, we presented a novel scheme to estimate the ambient temperature from the knowledge of the sensor characteristics itself, thus, eliminating the need for a separate temperature sensor. We have shown the effectiveness of the model in different forms of nonlinear influence of the ambient temperature on the pressure sensor characteristics with computer-simulated experiments.

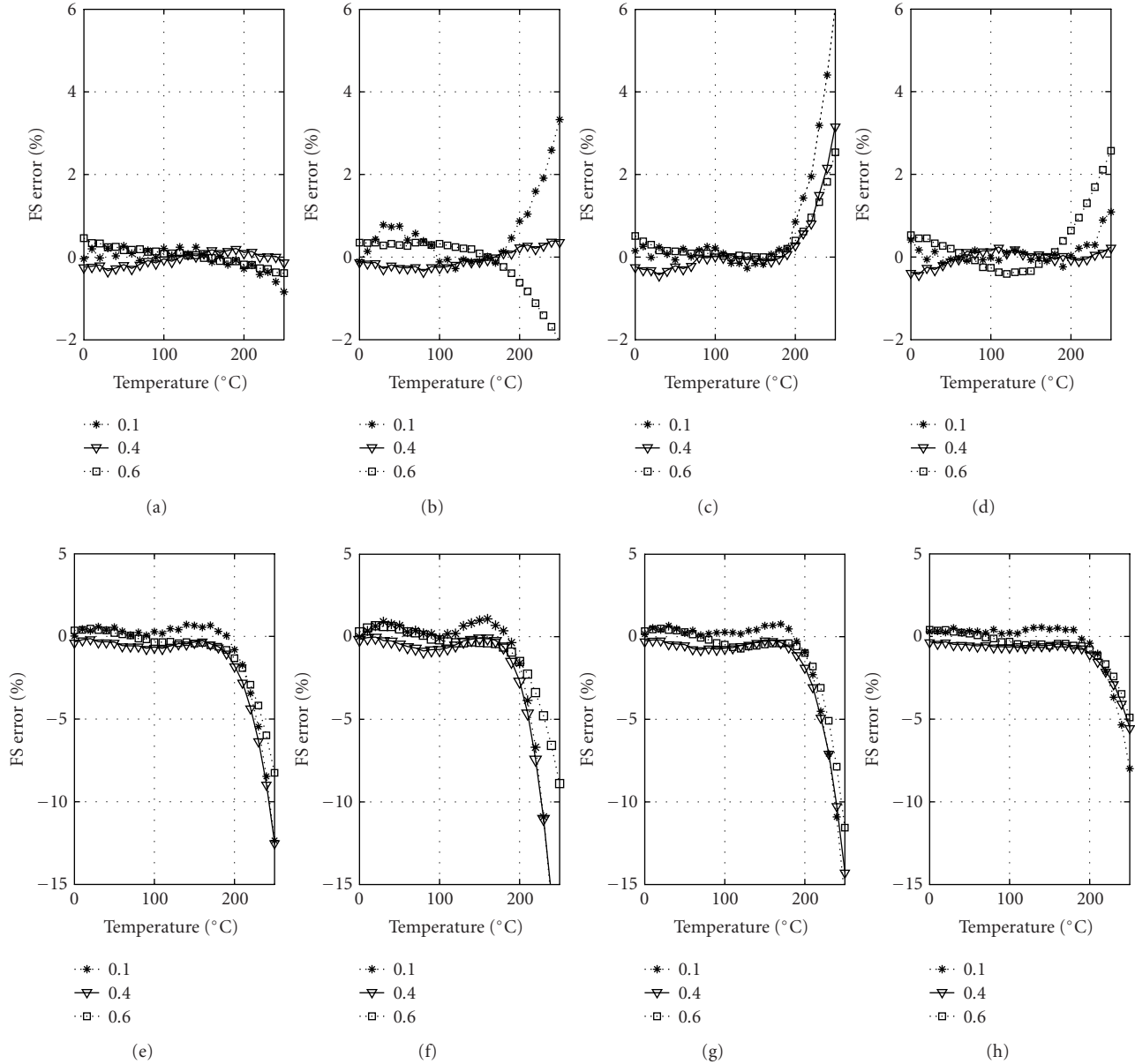


FIGURE 12: Full-scale percent error between the true and the estimated pressures at specific normalized pressures ($P_N = 0.1, 0.4,$ and 0.6) for the full range of variation of the ambient temperature. (a) and (e) NL0; (b) and (f) NL1; (c) and (g) NL2; and (d) and (h) NL3. The top row corresponds to the NN model and the bottom row corresponds to the polynomial model ($J = 5$). Both models were trained with $N_{\text{trgset}} = 4$.

TABLE 7: The MSE_{avg} for the polynomial model ($N_{\text{trgset}} = 4$ and $J = 5$) and the NN model with linear (NL0) and the three nonlinear temperature dependencies (NL1–NL3).

NL form	Temperature 0–250°C		Temperature 0–200°C	
	Poly. model	NN model	Poly. model	NN model
NL0	–30.01	–50.17	–45.33	–51.48
NL1	–25.02	–42.66	–42.97	–49.67
NL2	–28.11	–38.07	–44.87	–50.93
NL3	–34.70	–46.12	–46.19	–50.45

The performance of the NN model was compared with that of a polynomial interpolation scheme with a poly-

nomial degree of five (21 coefficients). It is shown that the NN-based model outperforms the polynomial model,

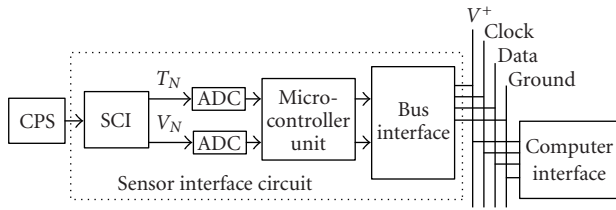


FIGURE 13: A scheme of a MCU-based implementation of the pressure sensor NN model.

especially for extrapolation of data. A scheme for an MCU-based implementation of the proposed NN-based models is also provided. Such NN-based models may be applied to other types of sensors to incorporate intelligence in terms of mitigating the nonlinear dependency of their response characteristics on the environmental parameters.

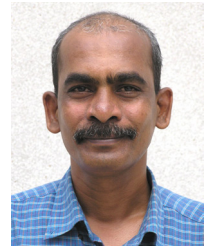
ACKNOWLEDGMENT

The authors would like to express their sincere thanks to the anonymous reviewers whose positive and constructive comments helped to enhance the quality and presentation of this paper.

REFERENCES

- [1] P. T. Kolen, "Self-calibration/compensation technique for microcontroller-based sensor arrays," *IEEE Trans. Instrum. Meas.*, vol. 43, no. 4, pp. 620–623, 1994.
- [2] P. Hille, R. Hohler, and H. Strack, "A linearisation and compensation method for integrated sensors," *Sensors and Actuators B*, vol. 44, no. 2, pp. 95–102, 1994.
- [3] M. Yamada and K. Watanabe, "A capacitive pressure sensor interface using oversampling Δ - Σ demodulation techniques," *IEEE Trans. Instrum. Meas.*, vol. 46, no. 1, pp. 3–7, 1997.
- [4] K. F. Lyahou, G. van der Horn, and J. H. Huijsing, "A non-iterative polynomial 2-D calibration method implemented in a microcontroller," *IEEE Trans. Instrum. Meas.*, vol. 46, no. 4, pp. 752–757, 1997.
- [5] X. Li, G. C. M. Meijer, and G. W. de Jong, "A microcontroller-based self-calibration technique for a smart capacitive angular-position sensor," *IEEE Trans. Instrum. Meas.*, vol. 46, no. 4, pp. 888–892, 1997.
- [6] G. Bucci, M. Faccio, and C. Landi, "New ADC with piecewise linear characteristic: case study-implementation of a smart humidity sensor," *IEEE Trans. Instrum. Meas.*, vol. 49, no. 6, pp. 1154–1166, 2000.
- [7] W. J. Kulesza, A. Hultgren, J. McGhee, M. Lennels, T. Bergander, and J. Wirandi, "An in-situ real-time impulse response auto test of resistance temperature sensors," *IEEE Trans. Instrum. Meas.*, vol. 50, no. 6, pp. 1625–1629, 2001.
- [8] S. Haykin, *Neural Networks*, Maxwell Macmillan, Ontario, Canada, 1994.
- [9] L. F. Pau and F. S. Johansen, "Neural network signal understanding for instrumentation," *IEEE Trans. Instrum. Meas.*, vol. 39, no. 4, pp. 558–564, 1990.
- [10] P. Daponte and D. Grimaldi, "Artificial neural networks in measurements," *Measurement*, vol. 23, no. 2, pp. 93–115, 1998.
- [11] J. M. Dias Pereira, P. M. B. Silva Girao, and O. Postolache, "Fitting transducer characteristics to measured data," *IEEE Instrum. Meas. Mag.*, vol. 4, no. 4, pp. 26–39, 2001.
- [12] J. C. Patra, G. Panda, and R. Baliarsingh, "Artificial neural network-based nonlinearity estimation of pressure sensors," *IEEE Trans. Instrum. Meas.*, vol. 43, no. 6, pp. 874–881, 1994.
- [13] J. C. Patra, A. C. Kot, and G. Panda, "An intelligent pressure sensor using neural networks," *IEEE Trans. Instrum. Meas.*, vol. 49, no. 4, pp. 829–834, 2000.
- [14] J. C. Patra, A. van den Bos, and A. C. Kot, "An ANN-based smart capacitive pressure sensor in dynamic environment," *Sensors and Actuators A*, vol. 86, no. 1-2, pp. 26–38, 2000.
- [15] J. M. Dias Pereira, O. Postolache, and P. M. B. Silva Girao, "A temperature-compensated system for magnetic field measurements based on artificial neural networks," *IEEE Trans. Instrum. Meas.*, vol. 47, no. 2, pp. 494–498, 1998.
- [16] A. Carullo, F. Ferraris, S. Graziani, U. Grimaldi, and M. Parvis, "Ultrasonic distance sensor improvement using a two-level neural-network," *IEEE Trans. Instrum. Meas.*, vol. 45, no. 2, pp. 677–682, 1996.
- [17] G. Y. Tian, "Design and implementation of distributed measurement systems using fieldbus-based intelligent sensors," *IEEE Trans. Instrum. Meas.*, vol. 50, no. 5, pp. 1197–1202, 2001.
- [18] P. Arpaia, P. Daponte, D. Grimaldi, and L. Michaeli, "ANN-based error reduction for experimentally modeled sensors," *IEEE Trans. Instrum. Meas.*, vol. 51, no. 1, pp. 23–30, 2002.

Jagdish C. Patra was born in Nabarangpur, Orissa, India, in 1957. He obtained his B.S. (with honours) and M.S. degrees, both in electronics and telecommunication engineering, from Sambalpur University, India, in 1978 and 1989, respectively. He received his Ph.D. degree in electronics and communication engineering from the Indian Institute of Technology, Kharagpur, in 1996. After the completion of his B.S. degree, he worked in various R&D, teaching, and government organizations for about 8 years. In 1987, he joined the Regional Engineering College, Rourkela, Orissa, as a Lecturer, where he was promoted to an Assistant Professor in 1990. In April 1999, he went to the Technical University, Delft, the Netherlands, as a Guest Teacher (Gast-docent) for six months. Subsequently, in October 1999, he joined the School of Electrical and Electronic Engineering (EEE), Nanyang Technological University (NTU), Singapore, as a Research Fellow. Currently, he is serving as an Assistant Professor in the School of Computer Engineering, NTU, Singapore. His research interests include intelligent signal processing using neural networks, fuzzy sets, and genetic algorithms in the area of data security, sensor networks, image processing, and bioinformatics. He is a Member of IEEE, USA, and Institution of Engineers, India.



Ee Luang Ang received her B.Eng. degree with honours in electrical engineering from the National University of Singapore in 1987, and the M.S. degree in electrical engineering from the University of Wisconsin-Madison in 1994. She is presently an Assistant Professor in the School of Computer Engineering, Nanyang Technological University, Singapore. Her teaching and research interests are in the areas of microprocessor applications, and image and signal processing.



Narendra S. Chaudhari received his B.Tech. (with distinction), M.Tech., and Ph.D. degrees from the Indian Institute of Technology, Mumbai, India, in 1981, 1983, and 1988, respectively. After completing his B.Tech. degree in electrical engineering, he worked on the design of microprocessor-based electronic controllers in the Electronic Controls Division of Larsen and Toubro Ltd, Mumbai, in 1981. After receiving his Ph.D. degree in computer engineering, he was involved in



graduate-level training for the defense scientists (Ministry of Defense, Government of India) till 1998. He was a Visiting Professor in Southern Cross University, NSW, Australia, and Freie Universität, Berlin. Currently, he is with School of Computer Engineering, Nanyang Technological University, Singapore, as an Associate Professor since 2001. His research interests are in the areas of neural networks, computational learning, and optimization algorithms. He has more than 100 research publications to his credit. He is a Fellow of Institution of Electronics and Telecommunication Engineers, India, Chartered Engineer of Institution of Engineers, India, Senior Member of Computer Society of India, and member of many professional societies, including Singapore Computer Society, and Pattern Recognition and Machine Intelligence Association, Singapore.

Amitabha Das obtained his B.Tech. degree with honours in electronics and electrical communication engineering from the Indian Institute of Technology, Kharagpur, and his Ph.D. degree in computer engineering from the University of California, Santa Barbara. He has been with the School of Computer Engineering, Nanyang Technological University, Singapore, since 1992, where he is currently an Associate Professor.



He is a Member of the IEEE Communications Society and the Singapore Computer Society. His research interests include wireless networks, security, and industrial application of machine learning techniques.

Special Issue on Advanced Video Technologies and Applications for H.264/AVC and Beyond

Call for Papers

The recently developed video coding standard H.264/MPEG-4 AVC significantly outperforms previous standards in terms of coding efficiency at reasonable implementation complexity and costs in VLSI realization. Real-time H.264 coders will be available very soon. Many applications, such as surveillance systems with multiple video channel recording, multiple channel video services for mobile devices, will benefit from the H.264 coder due to its excellent coding efficiency. The new video coding technology introduces new opportunities for video services and applications. However, advanced video coding is only one aspect for successful video services and applications. To enable successful new applications, additional technologies to cope with time-varying channel behaviors and diverse usage characteristics are needed. For serving multiple videos, some extended designs such as joint rate-distortion optimization and scheduling of multiple parallel video sessions are also required to achieve fair and robust video storage and delivery. For video surveillance systems, intelligent video content analysis and scalabilities in video quality, resolution, and display area, coupled with wireless transmission, can offer new features for the application. Finally, computational complexity reduction and low-power design of video codecs as well as content protection of video streams are particularly important for mobile devices.

The goal of this special issue is to discuss state-of-the-art techniques to enable various video services and applications on H.264/AVC technologies and their new developments.

Topics of interest include (but are not limited to):

- Video over DVB-H
- Error resilience of video over mobile networks
- Video delivery in multiuser environments
- Rate-distortion optimization for multiple video sources
- Multipath delivery of video streams
- Optimization of video codecs for quality improvement and power reduction
- Security and content protection of video streams
- Transcoding techniques
- Scalable video

- Other advanced video coding technologies
- Video quality measures

Authors should follow the EURASIP JASP manuscript format described at the journal site <http://asp.hindawi.com/>. Prospective authors should submit an electronic copy of their complete manuscript through the EURASIP JASP's manuscript tracking system at <http://www.mstracking.com/asp/>, according to the following timetable:

Manuscript Due	August 1, 2005
Acceptance Notification	November 1, 2005
Final Manuscript Due	March 1, 2006
Publication Date	3rd Quarter, 2006

GUEST EDITORS:

Jar-Ferr Yang, National Cheng Kung University, Tainan, Taiwan; jfyang@ee.ncku.edu.tw

Hsueh-Ming Hang, National Chiao Tung University, Hsinchu 300, Taiwan; h nhang@mail.ncku.edu.tw

Eckehard Steinbach, Munich University of Technology, Munich, Germany; eckehard.steinbach@tum.de

Ming-Ting Sun, University of Washington, Seattle, Washington, USA; sun@ee.washington.edu

Special Issue on Advances in Blind Source Separation

Call for Papers

Almost every multichannel measurement includes mixtures of signals from several underlying sources. While the structure of the mixing process may be known to some degree, other unknown parameters are necessary to demix the measured sensor data. The time courses of the source signals and/or their locations in the source space are often unknown a priori and can only be estimated by statistical means. In the analysis of such measurements, it is essential to separate the mixed signals before beginning postprocessing.

Blind source separation (BSS) techniques then allow separation of the source signals from the measured mixtures. Many BSS problems may be solved using independent component analysis (ICA) or alternative approaches such as sparse component analysis (SCA) or nonnegative matrix factorization (NMF), evolving from information theoretical assumptions that the underlying sources are mutually statistically independent, sparse, smooth, and/or nonnegative.

The aim of this special issue is to focus on recent developments in this expanding research area.

The special issue will focus on one hand on theoretical approaches for single- and multichannel BSS, evolving from information theory, and especially on nonlinear blind source separation methods, and on the other hand on their currently ever-widening range of applications such as brain imaging, image coding and processing, dereverberation in noisy environments, and so forth.

Authors should follow the EURASIP JASP manuscript format described at <http://www.hindawi.com/journals/asp/>. Prospective authors should submit an electronic copy of their complete manuscript through the EURASIP JASP manuscript tracking system at <http://www.mstracking.com/asp/>, according to the following timetable:

Manuscript Due	October 1, 2005
Acceptance Notification	February 1, 2006
Final Manuscript Due	May 1, 2006
Publication Date	3rd Quarter, 2006

GUEST EDITORS:

Scott Makeig, Swartz Center for Computational Neuroscience, Institute for Neural Computation, University of California, San Diego, La Jolla, CA 92093-0961, USA; smakeig@ucsd.edu

Andrzej Cichocki, Laboratory for Advanced Brain Signal Processing, Brain Science Institute, The Institute of Physical and Chemical Research (RIKEN), 2-1 Hirosawa, Wako, Saitama 351-0198, Japan; cia@brain.riken.go.jp

Frank Ehlers, Federal Armed Forces Underwater Acoustics and Marine Geophysics Research Institute, Klausdorfer Weg 2-24, 24148 Kiel, Germany; frankehlers@ieee.org

Special Issue on Tracking in Video Sequences of Crowded Scenes

Call for Papers

Object tracking in live video is an enabling technology that is in strong demand by large application sectors, such as video surveillance for security and behavior analysis, traffic monitoring, sports analysis for enhanced TV broadcasting and coaching, and human body tracking for human-computer interaction and movie special effects.

Many techniques and systems have been developed and demonstrated for tracking objects in video sequences. The specific goal of this special issue is to provide a status report regarding the state of the art in object tracking in crowded scenes based on the video stream(s) of one or more cameras. The objects can be people, animals, cars, and so forth. The cameras can be fixed or moving. Moving cameras may pan, tilt, and zoom in ways that may or may not be communicated to the tracking system.

All papers submitted must address at least the following two issues:

- Processing of live video feeds

For many applications in surveillance/security and TV sports broadcasting, the results of processing have value only if they can be provided to the end user within an application-defined delay. The submitted papers should present algorithms that are plausibly applicable to such incremental (“causal”) processing of live video feeds, given suitable hardware.

- Handling of crowded scenes

Crowded-scene situations range from relatively simple (e.g., players on a planar field in a soccer match) to very difficult (e.g., crowds on stairs in an airport or a train station). The central difficulties in crowded scenes arise from the constantly changing occlusions of any number of objects by any number of other objects.

Occlusions can be resolved to some degree using a single video stream. However, many situations of occlusion are more readily resolved by the simultaneous use of several cameras separated by wide baselines. In addition to resolving ambiguities, multiple cameras also ease the exploitation of 3D structure, which can be important for trajectory estimation or event detection.

Topics of interest include principles and evaluation of relevant end-to-end systems or important components thereof, including (but not limited to):

- Handling of occlusions in the image plane in single-camera scenarios
- Handling of occlusions in a world coordinate system (3D, possibly degenerated to 2D) in single- or multi-camera scenarios
- Fusion of information from multiple cameras and construction of integrated spatiotemporal models of dynamic scenes
- 3D trajectory estimation
- Tracking of multiple rigid, articulated, or nonrigid objects
- Automatic recovery of camera pose from track data
- Detection and recognition of events involving multiple objects (e.g., offside in soccer)

Papers must present a thorough evaluation of the performance of the system or method(s) proposed in one or more application areas such as video surveillance, security, sports analysis, behavior analysis, or traffic monitoring.

Authors should follow the EURASIP JASP manuscript format described at <http://www.hindawi.com/journals/asp/>. Prospective authors should submit an electronic copy of their complete manuscript through the EURASIP JASP manuscript tracking system at <http://www.mstracking.com/asp/>, according to the following timetable:

Manuscript Due	October 1, 2005
Acceptance Notification	February 1, 2006
Final Manuscript Due	May 1, 2006
Publication Date	3rd Quarter, 2006

GUEST EDITORS:

Jacques G. Verly, Department of Electrical Engineering and Computer Science, University of Liège (ULg), Sart Tilman, Building B28, 4000 Liège, Belgium; jacques.verly@ulg.ac.be



John MacCormick, Microsoft Research, Silicon Valley,
1065 La Avenida Mountain View, CA 94043, USA;
jmacc@microsoft.com

Stephen McKenna, Division of Applied Computing, Uni-
versity of Dundee, Dundee DD1 4HN, Scotland, UK;
stephen@computing.dundee.ac.uk

Justus H. Piater, Department of Electrical Engineering and
Computer Science, University of Liège (ULg), Sart Tilman,
Building B28, 4000 Liège, Belgium; justus.piater@ulg.ac.be

Special Issue on

Advances in Subspace-Based Techniques for Signal Processing and Communications

Call for Papers

Subspace-based techniques have been studied extensively over the past two decades and have proven to be very powerful for estimation and detection tasks in many signal processing and communications applications. Such techniques were initially investigated in the context of super-resolution parametric spectral analysis and the related problem of direction finding. During the past decade or so, new potential applications have emerged, and subspace methods have been proposed in several diverse fields such as smart antennas, sensor arrays, system identification, time delay estimation, blind channel estimation, image segmentation, speech enhancement, learning systems, and so forth.

Subspace-based methods not only provide new insight into the problem under investigation but they also offer a good trade-off between achieved performance and computational complexity. In most cases they can be considered as low cost alternatives to computationally intensive maximum likelihood approaches.

The interest of the signal processing community in subspace-based schemes remains strong as is evident from the numerous articles and reports published in this area each year. Research efforts are currently focusing on the development of low-complexity adaptive implementations and their efficient use in applications, numerical stability, convergence analysis, and so forth.

The goal of this special issue is to present state-of-the-art subspace techniques for modern applications and to address theoretical and implementation issues concerning this useful methodology.

Topics of interest include (but are not limited to):

- Efficient and stable subspace estimation and tracking methods
- Subspace-based detection techniques
- Sensor array signal processing
- Smart antennas
- Space-time, multiuser, multicarrier communications
- System identification and blind channel estimation
- State-space model estimation and change detection
- Learning and classification

- Speech processing (enhancement, recognition)
- Biomedical signal processing
- Image processing (face recognition, compression, restoration)

Authors should follow the EURASIP JASP manuscript format described at <http://www.hindawi.com/journals/asp/>. Prospective authors should submit an electronic copy of their complete manuscript through the EURASIP JASP manuscript tracking system at <http://www.mstracking.com/asp/>, according to the following timetable:

Manuscript Due	October 1, 2005
Acceptance Notification	February 1, 2006
Final Manuscript Due	May 1, 2006
Publication Date	3rd Quarter, 2006

GUEST EDITORS:

Kostas Berberidis, University of Patras, 26500 Patras, Greece; berberid@ceid.upatras.gr

Benoit Champagne, McGill University, Québec, Canada H3A 2T5; champagne@ece.mcgill.ca

George V. Moustakides, University of Thessaly, 38221 Volos, Greece; moustaki@uth.gr

H. Vincent Poor, Princeton University, Princeton, NJ 08544, USA; poor@princeton.edu

Peter Stoica, Uppsala University, 75105 Uppsala, Sweden; peter.stoica@it.uu.se

Special Issue on Image Perception

Call for Papers

Perception is a complex process that involves brain activities at different levels. The availability of models for the representation and interpretation of the sensory information opens up new research avenues that cut across neuroscience, imaging, information engineering, and modern robotics.

The goal of the multidisciplinary field of perceptual signal processing is to identify the features of the stimuli that determine their “perception,” namely “a single unified awareness derived from sensory processes while a stimulus is present,” and to derive associated computational models that can be generalized.

In the case of vision, the stimuli go through a complex analysis chain along the so-called “visual pathway,” starting with the encoding by the photoreceptors in the retina (low-level processing) and ending with cognitive mechanisms (high-level processes) that depend on the task being performed.

Accordingly, low-level models are concerned with image “representation” and aim at emulating the way the visual stimulus is encoded by the early stages of the visual system as well as capturing the varying sensitivity to the features of the input stimuli; high-level models are related to image “interpretation” and allow to predict the performance of a human observer in a given predefined task.

A global model, accounting for both such bottom-up and top-down approaches, would enable the automatic interpretation of the visual stimuli based on both their low-level features and their semantic content.

Among the main image processing fields that would take advantage of such models are feature extraction, content-based image description and retrieval, model-based coding, and the emergent domain of medical image perception.

The goal of this special issue is to provide original contributions in the field of image perception and modeling.

Topics of interest include (but are not limited to):

- Perceptually plausible mathematical bases for the representation of visual information (static and dynamic)
- Modeling nonlinear processes (masking, facilitation) and their exploitation in the imaging field (compression, enhancement, and restoration)

- Beyond early vision: investigating the pertinence and potential of cognitive models (feature extraction, image quality)
- Stochastic properties of complex natural scenes (static, dynamic, colored) and their relationships with perception
- Perception-based models for natural (static and dynamic) textures. Theoretical formulation and psychophysical validation
- Applications in the field of biomedical imaging (medical image perception)

Authors should follow the EURASIP JASP manuscript format described at <http://www.hindawi.com/journals/asp/>. Prospective authors should submit an electronic copy of their complete manuscripts through the EURASIP JASP manuscript tracking system at <http://www.mstracking.com/asp/>, according to the following timetable:

Manuscript Due	December 1, 2005
Acceptance Notification	April 1, 2006
Final Manuscript Due	July 1, 2006
Publication Date	3rd Quarter, 2006

GUEST EDITORS:

Gloria Menegaz, Department of Information Engineering, University of Siena, Siena, Italy; menegaz@dii.unisi.it

Guang-Zhong Yang, Department of Computing, Engineering Imperial College London, London, UK; gzy@doc.ic.ac.uk

Maria Concetta Morrone, Università Vita-Salute San Raffaele, Milano, Italy; concetta@in.cnr.it

Stefan Winkler, Genista Corporation, Montreux, Switzerland; stefan.winkler@genista.com

Javier Portilla, Department of Computer Science and Artificial Intelligence (DECSAI), Universidad de Granada, Granada, Spain; javier@decsai.ugr.es

Special Issue on Music Information Retrieval Based on Signal Processing

Call for Papers

The main focus of this special issue is on the application of digital signal processing techniques for music information retrieval (MIR). MIR is an emerging and exciting area of research that seeks to solve a wide variety of problems dealing with preserving, analyzing, indexing, searching, and accessing large collections of digitized music. There are also strong interests in this field of research from music libraries and the recording industry as they move towards digital music distribution. The demands from the general public for easy access to these music libraries challenge researchers to create tools and algorithms that are robust, small, and fast.

Music is represented in either encoded audio waveforms (CD audio, MP3, etc.) or symbolic forms (musical score, MIDI, etc.). Audio representations, in particular, require robust signal processing techniques for many applications of MIR since meaningful descriptions need to be extracted from audio signals in which sounds from multiple instruments and vocals are often mixed together. Researchers in MIR are therefore developing a wide range of new methods based on statistical pattern recognition, classification, and machine learning techniques such as the Hidden Markov Model (HMM), maximum likelihood estimation, and Bayes estimation as well as digital signal processing techniques such as Fourier and Wavelet transforms, adaptive filtering, and source-filter models. New music interface and query systems leveraging such methods are also important for end users to benefit from MIR research.

Although research contributions on MIR have been published at various conferences in 1990s, the members of the MIR research community meet annually at the International Conference on Music Information Retrieval (ISMIR) since 2000.

Topics of interest include (but are not limited to):

- Automatic summarization (succinct representation of music)
- Automatic transcription (audio to symbolic format conversion)
- Music annotation (semantic analysis)
- Music fingerprinting (unique identification of music)
- Music interface
- Music similarity metrics (comparison)

- Music understanding
- Musical feature extraction
- Musical styles and genres
- Optical music score recognition (image to symbolic format conversion)
- Performer/artist identification
- Query systems
- Timbre/instrument recognition

Authors should follow the EURASIP JASP manuscript format described at <http://www.hindawi.com/journals/asp/>. Prospective authors should submit an electronic copy of their complete manuscripts through the EURASIP JASP manuscript tracking system at <http://www.mstracking.com/asp/>, according to the following timetable:

Manuscript Due	December 1, 2005
Acceptance Notification	April 1, 2006
Final Manuscript Due	July 1, 2006
Publication Date	3rd Quarter, 2006

GUEST EDITORS:

Ichiro Fujinaga, McGill University, Montreal, QC, Canada, H3A 2T5; ich@music.mcgill.ca

Masataka Goto, National Institute of Advanced Industrial Science and Technology, Japan; m.goto@aist.go.jp

George Tzanetakis, University of Victoria, Victoria, BC, Canada, V8P 5C2; gtzan@cs.uvic.ca

Special Issue on Visual Sensor Networks

Call for Papers

Research into the design, development, and deployment of networked sensing devices for high-level inference and surveillance of the physical environment has grown tremendously in the last few years.

This trend has been motivated, in part, by recent technological advances in electronics, communication networking, and signal processing.

Sensor networks are commonly comprised of lightweight distributed sensor nodes such as low-cost video cameras. There is inherent redundancy in the number of nodes deployed and corresponding networking topology. Operation of the network requires autonomous peer-based collaboration amongst the nodes and intermediate data-centric processing amongst local sensors. The intermediate processing known as in-network processing is application-specific. Often, the sensors are untethered so that they must communicate wirelessly and be battery-powered. Initial focus was placed on the design of sensor networks in which scalar phenomena such as temperature, pressure, or humidity were measured.

It is envisioned that much societal use of sensor networks will also be based on employing content-rich vision-based sensors. The volume of data collected as well as the sophistication of the necessary in-network stream content processing provide a diverse set of challenges in comparison with generic scalar sensor network research.

Applications that will be facilitated through the development of visual sensor networking technology include automatic tracking, monitoring and signaling of intruders within a physical area, assisted living for the elderly or physically disabled, environmental monitoring, and command and control of unmanned vehicles.

Many current video-based surveillance systems have centralized architectures that collect all visual data at a central location for storage or real-time interpretation by a human operator. The use of distributed processing for automated event detection would significantly alleviate mundane or time-critical activities performed by human operators, and provide better network scalability. Thus, it is expected that video surveillance solutions of the future will successfully utilize visual sensor networking technologies.

Given that the field of visual sensor networking is still in its infancy, it is critical that researchers from the diverse disciplines including signal processing, communications, and electronics address the many challenges of this emerging field. This special issue aims to bring together a diverse set of research results that are essential for the development of robust and practical visual sensor networks.

Topics of interest include (but are not limited to):

- Sensor network architectures for high-bandwidth vision applications
- Communication networking protocols specific to visual sensor networks
- Scalability, reliability, and modeling issues of visual sensor networks
- Distributed computer vision and aggregation algorithms for low-power surveillance applications
- Fusion of information from visual and other modalities of sensors
- Storage and retrieval of sensor information
- Security issues for visual sensor networks
- Visual sensor network testbed research
- Novel applications of visual sensor networks
- Design of visual sensors

Authors should follow the EURASIP JASP manuscript format described at <http://www.hindawi.com/journals/asp/>. Prospective authors should submit an electronic copy of their complete manuscripts through the EURASIP JASP manuscript tracking system at <http://www.mstracking.com/asp/>, according to the following timetable:

Manuscript Due	December 1, 2005
Acceptance Notification	April 1, 2006
Final Manuscript Due	July 1, 2006
Publication Date	3rd Quarter, 2006



GUEST EDITORS:

Deepa Kundur, Department of Electrical Engineering,
Texas A&M University, College Station, Texas, USA;
deepa@ee.tamu.edu

Ching-Yung Lin, Distributed Computing Department,
IBM TJ Watson Research Center, New York, USA;
chingyung@us.ibm.com

Chun Shien Lu, Institute of Information Science, Academia
Sinica, Taipei, Taiwan; lcs@iis.sinica.edu.tw

Special Issue on Multirate Systems and Applications

Call for Papers

Filter banks for the application of subband coding of speech were introduced in the 1970s. Since then, filter banks and multirate systems have been studied extensively. There has been great success in applying multirate systems to many applications. The most notable of these applications include subband coding for audio, image, and video, signal analysis and representation using wavelets, subband denoising, and so forth. Different applications also call for different filter bank designs and the topic of designing one-dimensional and multidimensional filter banks for specific applications has been of great interest.

Recently there has been growing interest in applying multirate theories to the area of communication systems such as, transmultiplexers, filter bank transceivers, blind deconvolution, and precoded systems. There are strikingly many dualities and similarities between multirate systems and multicarrier communication systems. Many problems in multicarrier transmission can be solved by extending results from multirate systems and filter banks. This exciting research area is one that is of increasing importance.

The aim of this special issue is to bring forward recent developments on filter banks and the ever-expanding area of applications of multirate systems.

Topics of interest include (but are not limited to):

- Multirate signal processing for communications
- Filter bank transceivers
- One-dimensional and multidimensional filter bank designs for specific applications
- Denoising
- Adaptive filtering
- Subband coding
- Audio, image, and video compression
- Signal analysis and representation
- Feature extraction and classification
- Other applications

Authors should follow the EURASIP JASP manuscript format described at <http://www.hindawi.com/journals/asp/>. Prospective authors should submit an electronic copy of their

complete manuscripts through the EURASIP JASP manuscript tracking system at <http://www.mstracking.com/asp/>, according to the following timetable:

Manuscript Due	January 1, 2006
Acceptance Notification	May 1, 2006
Final Manuscript Due	August 1, 2006
Publication Date	4th Quarter, 2006

GUEST EDITORS:

Yuan-Pei Lin, Department of Electrical and Control Engineering, National Chiao Tung University, Hsinchu, Taiwan; ypl@mail.nctu.edu.tw

See-May Phoong, Department of Electrical Engineering and Graduate Institute of Communication Engineering, National Taiwan University, Taipei, Taiwan; smp@cc.ee.ntu.edu.tw

Ivan Selesnick, Department of Electrical and Computer Engineering, Polytechnic University, Brooklyn, NY 11201, USA; selesi@poly.edu

Soontorn Oraintara, Department of Electrical Engineering, The University of Texas at Arlington, Arlington, TX 76010, USA; oraintar@uta.edu

Gerald Schuller, Fraunhofer Institute for Digital Media Technology (IDMT), Langewiesener Strasse 22, 98693 Ilmenau, Germany; shl@idmt.fraunhofer.de

Special Issue on Signal Processing with High Complexity: Prototyping and Industrial Design

Call for Papers

Some modern applications require an extraordinary large amount of complexity in signal processing algorithms. For example, the 3rd generation of wireless cellular systems is expected to require 1000 times more complexity when compared to its 2nd generation predecessors, and future 3GPP standards will aim for even more number-crunching applications. Video and multimedia applications do not only drive the complexity to new peaks in wired and wireless systems but also in personal and home devices. Also in acoustics, modern hearing aids or algorithms for de-reverberation of rooms, blind source separation, and multichannel echo cancellation are complexity hungry. At the same time, the anticipated products also put on additional constraints like size and power consumption when mobile and thus battery powered. Furthermore, due to new developments in electroacoustic transducer design, it is possible to design very small and effective loudspeakers. Unfortunately, the linearity assumption does not hold any more for this kind of loudspeakers, leading to computationally demanding nonlinear cancellation and equalization algorithms.

Since standard design techniques would either consume too much time or do not result in solutions satisfying all constraints, more efficient development techniques are required to speed up this crucial phase. In general, such developments are rather expensive due to the required extraordinary high complexity. Thus, de-risking of a future product based on rapid prototyping is often an alternative approach. However, since prototyping would delay the development, it often makes only sense when it is well embedded in the product design process. Rapid prototyping has thus evolved by applying new design techniques more suitable to support a quick time to market requirement.

This special issue focuses on new development methods for applications with high complexity in signal processing and on showing the improved design obtained by such methods. Examples of such methods are virtual prototyping, HW/SW partitioning, automatic design flows, float to fix conversions, automatic testing and verification, and power aware designs.

Authors should follow the EURASIP JES manuscript format described at <http://www.hindawi.com/journals/es/>. Prospective authors should submit an electronic copy of their complete manuscripts through the EURASIP JES's manuscript tracking system at <http://www.mstracking.com/es/>, according to the following timetable:

Manuscript Due	December 1, 2005
Acceptance Notification	March 1, 2006
Final Manuscript Due	June 1, 2006
Publication Date	3rd Quarter, 2006

GUEST EDITORS:

Markus Rupp, TU Wien, Gusshausstr. 25/389, A-1040 Wien, Austria; mrupp@nt.tuwien.ac.at

Thomas Kaiser, University of Duisburg-Essen, 47057 Duisburg, Germany; thomas.kaiser@uni-duisburg.de

Gerhard Schmidt, Harman Becker / Temic-SDS, Germany; gerhard.schmidt@temic-sds.com

Jean-Francois Nezan, IETR/Image group Lab, France; jean-francois.nezan@insa-rennes.fr